2005-06-15

Condition Analysis of Concrete Bridge Decks in Utah

Robert S. Tuttle
Brigham Young University - Provo

CONDITION ANALYSIS OF CONCRETE BRIDGE DECKS IN UTAH

by

Robert S. Tuttle

A thesis submitted to the faculty of

Brigham Young University

in partial fulfillment of the requirements for the degree of

Master of Science

Department of Civil and Environmental Engineering

Brigham Young University

August 2005

BRIGHAM YOUNG UNIVERSITY

GRADUATE COMMITTEE APPROVAL

of a thesis submitted by

Robert S. Tuttle

This thesis has been read by each member of the following graduate committee and by majority vote has been found to be satisfactory.

Date	W. Spencer Guthrie, Chair
Date	Fernando S. Fonseca
Date	Mitsuru Saito

BRIGHAM YOUNG UNIVERSITY

As chair of the candidate's graduate committee, I have read the thesis of Robert S. Tuttle in its final form and have found that (1) its format, citations, and bibliographical style are consistent and acceptable and fulfill university and department style requirements; (2) its illustrative materials including figures, tables, and charts are in place; and (3) the final manuscript is satisfactory to the graduate committee and is ready for submission to the university library.

Date

W. Spencer Guthrie
Chair, Graduate Committee

Accepted for the Department

A. Woodruff Miller
Department Chair

Accepted for the College

Alan R. Parkinson
Dean, Ira A. Fulton College of Engineering and Technology

ABSTRACT

CONDITION ANALYSIS OF CONCRETE BRIDGE DECKS IN UTAH

Robert S. Tuttle

Department of Civil and Environmental Engineering

Master of Science

Concrete bridge decks in Utah are experiencing observable deterioration due primarily to freeze-thaw cycles and the routine application of deicing salts during winter maintenance activities. Given the need for increasingly cost-effective strategies for bridge deck maintenance, rehabilitation, and replacement (MR&R), the Utah Department of Transportation (UDOT) initiated this research to ultimately develop a protocol offering guidance as to whether deteriorated bridge decks should be rehabilitated or replaced. While threshold values for various non-destructive condition assessment methods were proposed in earlier UDOT research, this work focused on implementing the recommended test criteria. Twelve bridges were identified by UDOT engineers for inclusion in the study, and data were collected from each deck to determine whether the bridge decks warranted rehabilitation or replacement based on the proposed threshold values.

Several evaluation techniques were employed to assess concrete bridge deck condition, including visual inspection, hammer sounding and chaining, dielectric measurements, ground-penetrating radar imaging, resistivity testing, half-cell potential

testing, and chloride concentration testing. The condition assessment testing confirmed that chloride-induced corrosion of reinforcing steel is the primary mechanism of deck deterioration and that inadequate cover over the upper steel mat facilitated accelerated corrosion damage in many instances. The bridge deck condition analyses produced from the results of non-destructive testing were compared to the visual inspection ratings assigned to each deck by UDOT.

Concrete bridge deck condition data should be collected regularly through inspection and monitoring programs to facilitate prioritization of MR&R strategies for individual bridges and to evaluate the impact of such strategies on the overall condition of the network. Performance indices based on selected condition assessment parameters should be developed for use in bridge management activities, and mathematical deterioration models should be calibrated in order to forecast both network-level and project-level conditions and predict funding requirements for various possible MR&R strategies. Further research, including statistical analyses of the data presented in this report, should be completed to develop relevant mathematical deterioration models for predicting the service lives of concrete bridge decks in Utah.

ACKNOWLEDGMENTS

The author wishes to acknowledge Daniel Hsiao of UDOT for directing this project and coordinating communication between UDOT and Brigham Young University (BYU). Appreciation is also given to Mike Ellis of UDOT for arranging traffic control during the bridge deck testing. UDOT bridge engineers David Nazare, Todd Jensen, David Eixenberger, and Boyd Wheeler served on the technical advisory committee for this project. Graduate research assistants Brandon Blankenagel, Ashley Brown, Dane Cooley, Jon Hanson, Russell Lay, and Tyler Nelsen assisted in the bridge deck testing required for this research. In addition, my wife and family have given me tremendous support to accomplish this part of my education.

TABLE OF CONTENTS

LIST OF TABLES

LIST OF FIGURES

CHAPTER 1
INTRODUCTION

1.1 PROBLEM STATEMENT

The aging and deterioration of bridges in Utah mandates increasingly cost-effective strategies for bridge maintenance, rehabilitation, and replacement (MR&R). The 2004 national bridge inventory (NBI) report indicates that of the 2,992 bridges in Utah, 8.6 percent are structurally deficient, and an additional 8.5 percent are functionally obsolete. The NBI report also indicates that 86.7 percent of Utah bridges are recommended to have some structural portion of the bridge, or the entire bridge, replaced due to substandard load-carrying capacity or substandard bridge roadway geometry. The cost to provide the necessary MR&R improvements for bridges in Utah, according to the NBI report, is estimated to exceed $1.4 billion (*1*).

The Utah Department of Transportation (UDOT) is responsible for 1,700 bridges throughout the state, of which 46 percent are older than 30 years as shown in Figure 1.1 (*2*). Utah cities and counties, as well as the federal government, hold responsibility for the remaining 1,292 bridges. Due to the comparatively high number of state-owned bridges approaching the end of their service lives, UDOT engineers are interested in developing a protocol for objectively and reliably assessing the condition of concrete bridge decks in order to optimize MR&R actions.

The research documented in this report focused on implementing the recommended test criteria established in earlier UDOT research performed at Brigham Young University (BYU) (*2*). The criteria were based on various non-destructive condition assessment methods with associated threshold values. Because the previous research identified corrosion of reinforcing steel as the primary cause of concrete bridge deck damage, this research investigated non-destructive testing techniques that

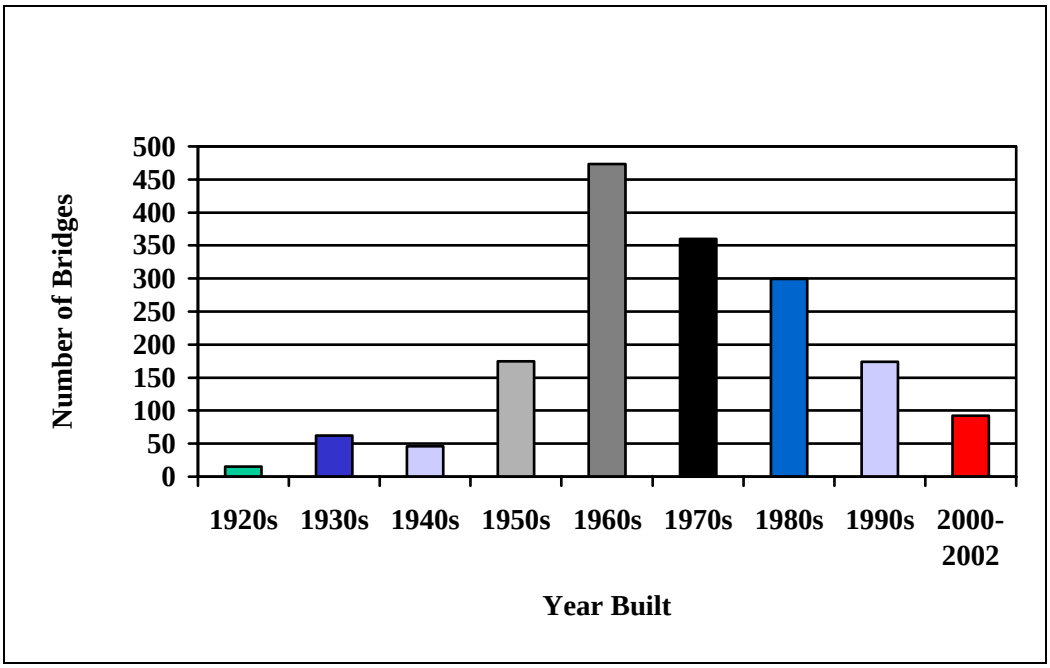

FIGURE 1.1 Bridge construction in Utah since 1920 (*2*).

can be used to estimate the extent of corrosion activity occurring within the deck before damage is visually apparent on the deck surface in the form of cracking, delaminations, or potholes. In consultation with UDOT engineers, the research team selected 12 bridges for inclusion in this study, and data were collected from each bridge deck to determine whether the bridge decks warranted rehabilitation or replacement based on the proposed threshold values.

1.2 SCOPE

Research performed in this study considered 12 concrete bridge decks of various age and condition, all generally located in northern Utah. Certified UDOT officials conduct bridge inspections for the concrete decks every two years. Although a typical inspection report provides information for all of the components of a bridge, this study considered only the bridge deck. Inspection reports from selected bridges in this research were used in conjunction with the results of non-destructive testing to establish the condition and corrosion potential of the bridge decks. Depending on the extent and severity of

deterioration manifested on each deck, a recommendation to rehabilitate or replace each tested bridge deck is provided.

The non-destructive testing methods used by BYU researchers were selected based on an extensive literature review and a questionnaire survey of departments of transportation (DOTs) nationwide (*2*). The condition assessment methods used in this research included visual inspection, hammer sounding and chaining, dielectric measurements, ground-penetrating radar (GPR) imaging, resistivity testing, half-cell potential testing, and chloride concentration measurements. The bridge deck condition analyses from the non-destructive testing were compared to the visual inspection ratings assigned to each deck by UDOT inspectors.

The data collected from this research may be useful for developing numerical deterioration models for predicting future bridge deck condition; however, development of such models is beyond the scope of the present work.

1.3 OUTLINE OF REPORT

This report contains five chapters. Chapter 1 presented the objectives and scope of the research. In Chapter 2 the purpose and benefits of a bridge management system (BMS) are presented. A description of the theory and procedures associated with each of the non-destructive tests used for collecting data is given in Chapter 3. Test results and a summary of bridge deck inspections completed by UDOT officials are presented in Chapter 4, together with recommendations about whether each bridge deck should be rehabilitated or replaced. In Chapter 5 a summary of the procedures, research findings, and recommendations for further research is presented.

CHAPTER 2
BRIDGE MANAGEMENT SYSTEMS

2.1 PURPOSE AND BENEFITS

The overall aim of a BMS is to maximize the average service life of bridges through scheduled maintenance and repairs, where the service life of a bridge is the time between construction and replacement. A BMS allows decision-makers at all bridge management levels to select optimum solutions from a variety of cost-effective alternatives that should deliver the desired level of service while minimizing the overall life-cycle cost of a bridge (*2*).

The steps and objectives of a BMS include the following (*3*):

- predict bridge needs
- define bridge conditions
- allocate funds for both construction and MR&R actions
- identify and prioritize bridges for MR&R actions
- identify bridges that require a load posting
- find cost-effective alternatives for each bridge
- recommend and account for MR&R actions
- schedule and perform minor maintenance
- monitor and rate bridges
- maintain an appropriate database of information

Conditions of specific bridge elements can be analyzed with BMS software to assist in funding distribution and bridge MR&R prioritization. One such computer-based system, PONTIS, was developed under a Federal Highway Administration (FHWA) project and is available through the American Association of State Highway and Transportation Officials (AASHTO) (*4*). PONTIS supports a string of activities, including information-

gathering and interpretation, prediction of bridge conditions, cost accounting, decision-making, budgeting, and planning. The software systematically addresses each of these factors to facilitate prediction of future bridge condition, cost estimation, and comparison of possible actions. Like most computer-based management systems, PONTIS relies on mathematical assumptions to generate life-cycle predictions. Although transportation agency employees, such as UDOT engineers, are not required to understand the mathematical models used in the software, they should clearly understand the significance of the projections.

Routine analysis of bridge condition information is an essential operational component of a BMS (*3*). The collection and storage of bridge inventory, condition, and MR&R data are the basis by which bridges are analyzed and selected for rehabilitation or replacement. Data collection should be limited to information that contributes directly to an accurate life-cycle cost analysis and objectives of the BMS. Excess data make the system less manageable, more expensive, and less accurate and, in fact, is the principal reason for the abandonment of most BMSs (*5*). Therefore, data collected in the development of a BMS should be useful for at least one of the following reasons (*6*):

- identifying bridges or decks with poor performance
- establishing priority
- selecting maintenance or rehabilitation actions
- calculating the cost of maintenance or rehabilitation actions
- estimating life-cycle costs for each maintenance and rehabilitation action

Additional information may be collected, but the criteria for selection should consider how the information would be used in the BMS and the purpose that the information would serve the agency.

2.2 BRIDGE INSPECTION DATA

As required by the NBI program, bridge inspections are conducted by state DOTs every two years. In Utah, data collected from the inspections are compiled in two documents, the Structural Inventory and Appraisal Sheet and the UDOT Bridge Inspection Report. According to the UDOT Bridge Inspection Report, condition assessment of a bridge deck addresses the wearing surface, structural condition, expansion joints, railing, fencing,

sidewalks, curbs, and median. Evaluation of the wearing surface includes the surface type, top surface condition, and overall thickness. The structural condition assessment considers the condition of the top and bottom surfaces of the deck and the overhangs. Assessment of the expansion joints includes the joint type and the occurrence of any leakage. The deck is then assigned a condition assessment score from 0 to 9, as shown in Table 2.1 (*7*). In addition to the deck condition rating, observations of visual distresses manifested on the bridge deck are also included in the report. PONTIS can then be used to analyze and prioritize the MR&R needs of the bridge deck based on the deck condition rating.

Although some bridge decks may not exhibit any significant visual distress, the reinforcing steel in the concrete decks may be actively corroding. In these cases, the appropriate time for application of preventive maintenance treatments has passed, as the corroding rebar will inevitably lead to future distress regardless of any treatment applied to the deck; the engineers responsible for maintaining such bridges should then focus on potential rehabilitation or replacement strategies instead. In order to optimize applications of preventive maintenance treatments to bridge decks, engineers must monitor internal deck conditions and initiate preventive action before corrosion of the reinforcing steel begins. Evaluation, therefore, requires testing beyond even thorough visual inspections. For example, resistivity testing, half-cell potential testing, and

TABLE 2.1 Bridge Deck Condition Rating (*7*)

Score	Description
9	Excellent
8	Very Good
7	Good
6	Satisfactory
5	Fair
4	Poor
3	Serious
2	Critical
1	Imminent Failure
0	Failed

chloride concentration measurements can be employed to assess the internal deck condition, or the potential for corrosion and deterioration, of a given bridge deck.

2.3 FACTORS AFFECTING BRIDGE DECK CONDITION

In addition to construction quality and traffic loading, factors affecting the performance of concrete bridge decks in northern climates include winter applications of deicing salts and freeze-thaw cycles. Proximity to saline environments is also an important factor. Furthermore, the durability of concrete bridge decks is greatly dependent upon the quality of the concrete and the condition of the reinforcing steel.

The type of concrete and the quality of concrete placement determine the wear resistance and soundness of a concrete bridge deck. Soundness is the degree to which the concrete exhibits a uniform, consistent matrix free of defect, decay, and damage (*8*). The level of soundness reflects the ability of the concrete to resist deteriorative distresses such as cracking, delaminations, scaling, popouts, potholes, and infiltration of chlorides and other corrosive materials. In addition, the soundness of the matrix is generally indicative of the amount of voids and free water in the concrete; higher void contents are generally associated with lower concrete strengths and greater concrete permeability, both characteristics of poor-quality concrete. The soundness of the concrete and the thickness of the concrete clear cover control the rate at which air, water, deicing salts, and other harmful substances reach the steel reinforcement embedded in the concrete bridge deck. Bridge engineers should ensure that the actual clear cover depth is at least equal to that specified in design.

Cracking, one of the most unavoidable distresses in concrete, promotes deeper penetration of corrosive elements. Cracks that propagate to the level of the reinforcement can directly expose the steel to corrosive deicing salts, for example. Corrosion of steel produces rust, which is four to seven times greater in volume than the parent steel (*9*); therefore, the expansion associated with rust formation introduces bursting stresses and eventually leads to further cracking, delaminations, spalling, and potholes. The repeating cycle of cracking, chloride penetration, and steel corrosion is one of the leading causes of bridge deck deterioration.

In order to enhance bridge deck durability, many bridge design engineers specify the use of epoxy-coated steel reinforcement. The epoxy coating protects the steel from exposure to air, water, chlorides, and other elements that lead to corrosion. As long as it remains intact, the coating effectively creates an electrical barrier that prevents current flow between the steel reinforcement and the concrete, thus inhibiting the corrosion process. If the epoxy coating deteriorates, however, the exposed steel can become subject to corrosion. BMSs can be used to document and investigate the effect of such design and construction innovations on the overall performance of concrete bridge decks or other bridge components.

2.4 PREDICTIVE DETERIORATION MODELS

Deterioration models can be developed to estimate the service life of bridge decks as a function of relevant factors such as current deck condition, potential for corrosion, and frequency of exposure to corrosive elements. Because the service life of the substructure and superstructure of a bridge is estimated to be two to three times longer than that of a bridge deck, MR&R actions are necessary to extend the service life of the bridge deck before replacement is necessary. The diagram in Figure 2.1 shows the effects of MR&R intervention on the service life of a bridge deck (*10*). The condition index on the vertical axis of the deterioration model could represent one or more measurements of the bridge deck.

Four types of MR&R intervention exist to increase the service life of a bridge deck. These include preventive maintenance, corrective maintenance, rehabilitation, and replacement. Preventive, or proactive, maintenance should be implemented to retard deterioration before damage to the bridge deck has occurred. Such maintenance takes place during Phase I in the diagram, before any severe deterioration has occurred. Currently, many DOTs use a reactive, or corrective, approach to maintain the quality and life of a bridge deck. This type of maintenance is often employed on a regular basis throughout all phases of deterioration to preserve bridge decks at satisfactory operational condition. Rehabilitation is applied to restore the bridge decks

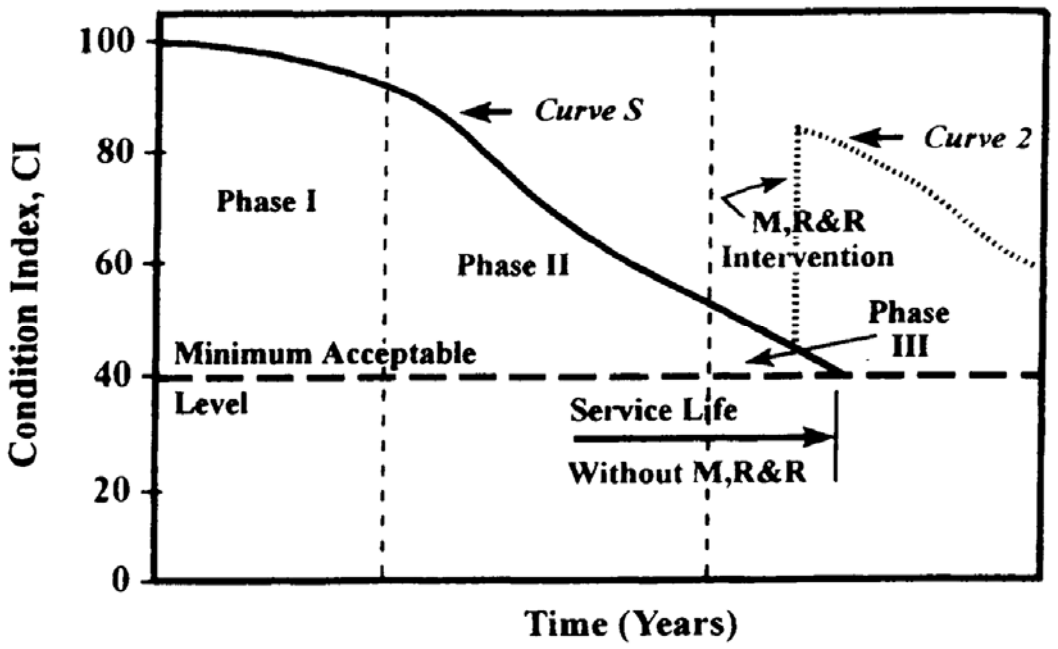

FIGURE 2.1 Effects of MR&R on bridge deck service life (*10*).

to their original state and takes place during Phase II in the diagram. Replacement, which demands the demolition and reconstruction of the entire bridge deck, takes place during Phase III, or when a bridge deck reaches the end of its service life by failing to sustain satisfactory conditions (*10*).

Both rehabilitation and replacement can be substantially postponed by effective application of preventive and reactive maintenance. An accurate deterioration model is necessary to ensure that all maintenance actions are applied effectively. Ultimately, development of predictive models like the one shown in Figure 2.1 would enhance the ability of DOT engineers to optimally schedule such MR&R treatments.

Deterioration models can be calibrated for a variety of applications. For instance, due to variability in construction practices, geographic location, and existing bridge deck condition, different models may be needed to represent different groups or classes of bridge decks. In addition, analysis of deterioration models may suggest a need to inspect bridges more or less frequently than the minimal requirement of two years established by the NBI system. Deterioration models may also be used as a basis for selecting the types

and extent of testing to be performed. In all cases, data collected during bridge deck inspections should be used to improve the accuracy of the models.

Given the capabilities of modern computers, collected data may be readily compiled into a searchable database. The database should be capable of searching through existing data in order to find all bridge decks with similar conditions. This type of search permits the user to identify all bridge decks requiring similar MR&R actions. The software should also have the capability to predict the condition of a specific bridge or the overall network if certain MR&R strategies are performed. In the latter case, the database would allow analyses of customized scenarios to predict future conditions of bridge decks based on proposed MR&R actions.

In order to increase the probability of a successful BMS, only qualified and trained personnel should enter and analyze collected data, even though the software should be user-friendly. Furthermore, a successful bridge inspection program may require the acquisition of new equipment, extensive training of bridge inspectors, enhancement of existing databases, and other related tasks. Despite the additional cost associated with these activities, a functional BMS should pay for itself relatively quickly by offering engineers more accurate information regarding the scheduling of MR&R actions for bridges within their jurisdictions.

CHAPTER 3
BRIDGE DECK TESTING PROCEDURES

3.1 INTRODUCTION

This chapter describes several non-destructive tests that have been developed for assessing the condition of concrete bridge decks. Condition assessment methods were selected for use in this project based on an extensive literature review and a questionnaire survey of state DOTs nationwide (*2*). The tests include visual inspection, hammer sounding and chaining, dielectric measurements, GPR imaging, resistivity testing, half-cell potential testing, and chloride concentration testing. The time, temperature, and relative humidity corresponding to each bridge deck evaluation were also recorded. The procedures and a brief description of the theory associated with each selected method of data collection are described in the following sections.

3.2 DECK TEST SECTION

The test area was chosen by examining the bridge deck and selecting a representative 100-ft by 10-ft section on the top surface of the deck. After sweeping the selected area, as shown in Figure 3.1, researchers painted station markers spaced at 5-ft intervals on the deck surface and labeled them with numerals between 0 and 20, as shown in Figure 3.2. Station markers were referenced to a fixed structure of the bridge, such as a specific deck joint or parapet feature. A prepared test area is shown in Figure 3.3.

FIGURE 3.1 Sweeping the test area.

FIGURE 3.2 Stationing the test area.

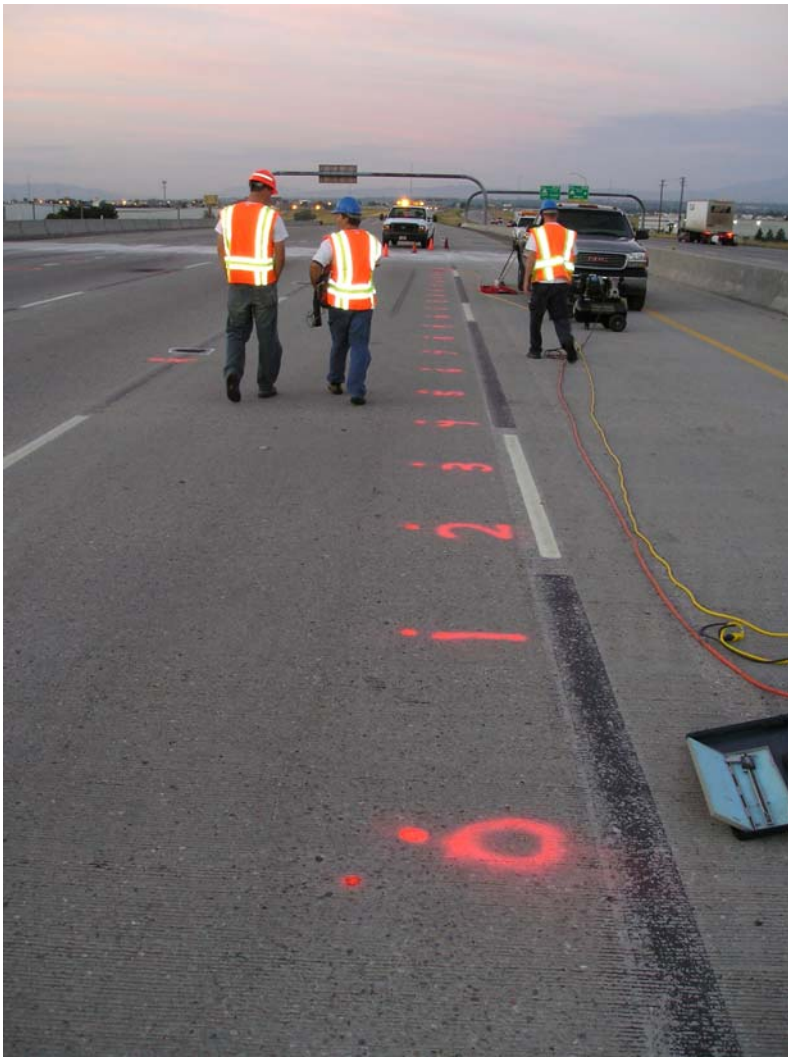

FIGURE 3.3 Prepared test area.

Visual inspection and sounding included a survey of the test area only, not the entire deck surface. However, photographs of distresses outside the test area were occasionally taken to more thoroughly document the overall deck condition. One dielectric measurement was taken at each station marker within the test area, and GPR imaging was performed along a linear, longitudinal profile of the deck, usually in line with the station markers painted within the test area. In addition, two resistivity and two half-cell potential readings were taken at each station marker, and one or two chloride concentration test holes were drilled in each deck, with holes located at either station 0 or station 20 or both. Figure 3.4 displays the typical locations of GPR,

dielectric, resistivity, half-cell potential, and chloride concentration tests performed on each deck. Visual inspection and sounding investigations were performed over the entire testing area.

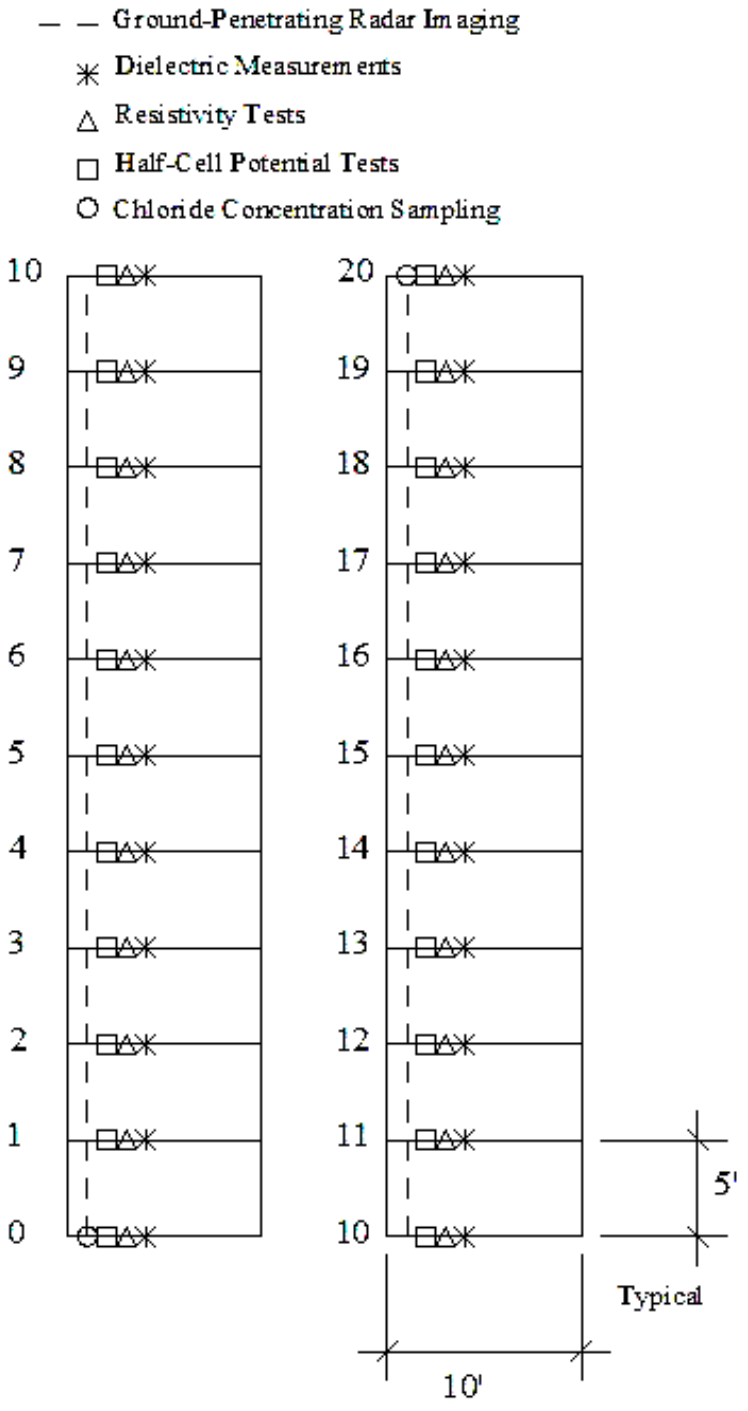

FIGURE 3.4 Typical location of tests performed on the bridge decks.

3.3 VISUAL INSPECTION

Visual inspection is the first step in assessing the condition of tested bridge decks and typically considers all distresses manifest on both the top and bottom surfaces of the decks (*11, 12*). In this research, the type and extent of deterioration within the test area were recorded on a distress map worksheet. Photographs were also taken of the bridge deck to document any significant damage and distresses characteristic of the deck. Photography was generally limited to documentation of distresses on the top surfaces of the tested decks since the undersides of the decks were not readily accessible.

Cracks are the precursors of more advanced bridge deck deterioration and were therefore among the most important visual features to document. Cracks were identified by their size, location, and orientation (*11*). Both the lengths and widths of visible cracks were recorded, where the crack width was measured using a crack width comparator card (*13*). Crack widths were categorized into four general groups: hairline, narrow, medium, or wide as summarized in Table 3.1 (*11*). Cracks that mirror the location of reinforcing steel can cause accelerated corrosion due to the greater ease with which chlorides, water, and oxygen can penetrate the concrete cover of the deck (*14*).

For bridge decks overlaid with a protective asphalt, epoxy, or polymer wearing surface, the apparent condition of the overlay surface may not have been an accurate representation of the actual deck condition. For example, when a waterproofing overlay is used, the concrete deck may be in excellent condition while the wearing surface may exhibit extensive deterioration (*11*). Conversely, the wearing surface may

TABLE 3.1 Crack Width Categories (*11*)

Category	Crack Width (in.)
Hairline	< 0.004
Narrow	0.004 to 0.01
Medium	0.01 to 0.03
Wide	> 0.03

be in good condition while the concrete deck is heavily deteriorated (*11*). While removal of wearing surfaces may be desirable to facilitate more accurate deck evaluations in extreme cases, the asphalt overlay on just one deck was removed for this testing.

In this research, visual distress data were used to formulate three types of deck condition descriptors, including crack density, crack severity, and pothole density. Crack density reports the lineal footage of cracking per square yard of concrete surface area within the test section and was calculated by dividing the sum of total length of cracking in feet by the total area of the survey section in square yards. Crack severity reports the average crack width, in inches, observed in the test section of the bridge deck. Pothole density compares the total area of potholes to the total area of the test section and was calculated as the ratio of total pothole distress area in square inches to the total area of the survey section in square yards. These parameters generated from visual inspection data therefore represent the test area only.

Although many state DOTs use these and other similar descriptors to determine optimum deck improvement strategies, standard threshold values have yet to be established for general use. Nevertheless, responses to the questionnaire survey mentioned earlier indicate that most DOTs recommend maintenance action when crack widths exceed 0.0625 in. with moderate crack density or when efflorescence is evident in the vicinity of the cracks (*2*). According to AASHTO, if 10 to 50 percent of the deck area is affected by potholes, deck repairs need to be implemented (*2*).

3.4 CHAIN DRAGGING AND HAMMER SOUNDING

Chain dragging and hammer sounding were used to locate subsurface delaminations within the test area of each bridge deck. A heavy steel chain was dragged across the bridge deck surface within the test area, and the operator listened to changes in the acoustic response of the bridge deck. Good quality concrete produced a clear ringing sound, while the acoustic response for delaminations was a dull, hollow sound (*13*, *15*).

Although chain dragging effectively locates delaminations, it is not a reliable method for directly identifying areas of corroding reinforcement (*15*). Also, because

different operators hear the same sound differently, chain dragging is a subjective evaluation method. Another disadvantage of chain dragging is its inability to detect early-age delaminations. Most delaminations detectable by chain dragging have progressed to the point where major rehabilitation is required (*16*). Chain dragging also does not allow the operator to accurately detect delaminations on asphalt-covered decks. While the method was used effectively on thin polymer or epoxy overlays in this research, the chain should be in direct contact with the concrete surface for optimum results (*6*). Nonetheless, the relatively low cost and speed at which chain dragging can be performed made it useful as a deck condition assessment method in this project (*11*).

In addition to chaining, hammer sounding was also utilized in this research to locate delaminations within the test area on each deck. The operator struck the concrete with a standard carpentry hammer and listened to the response (*13*, *17*). In this respect, the same limitations that applied to chain dragging applied to hammer sounding, including the subjective judgment and hearing sense of the operator (*11*, *17*). In addition, hammer sounding was slower and more tedious than chain dragging because only small areas of concrete could be analyzed at one time.

In some cases, the research team members used an iron bar dropped on its end, from an upright position, to perform sounding (*11*). The iron bar served as a wave-conducting device to transmit acoustic responses up the bar into the vicinity of the technician's ear. In this research, ringing of the bar often masked the differences in acoustical responses between intact and delaminated concrete; therefore, this method was only performed on a small number of bridge decks. Thus, only the locations of delaminations detected by way of chain dragging and hammer sounding were documented, and the actual size of the delaminations was estimated for only one bridge deck. According to most DOTs, maintenance of delaminations is recommended if 5 to 20 percent of the deck is affected, while AASHTO recommends maintenance of the deck if 10 to 50 percent is affected by delaminations (*2*).

3.5 DIELECTRIC MEASUREMENTS

The dielectric value of concrete reflects its ability to store an electrical charge and is dependent on its composition and microstructure (*17*). While the dielectric value of air is 1 and the dielectric value of solid aggregate particles generally ranges between 4 and 6, the dielectric value of free water is 81 (*18*). Therefore, the dielectric value of any three-phase mixture of these components will be most sensitive to the presence of water. Because increasing concrete porosity is usually associated with greater amounts of free water entrapped within the concrete matrix, the dielectric values of porous, moist concrete usually exceed the dielectric values of low-permeability concrete.

In this research, dielectric values were measured at the surface of the concrete using an Adek Percometer device operating at a frequency of 50 MHz. Figure 3.5 shows the device being used to measure dielectric values for one of the bridge decks. A single dielectric measurement was taken at each station in the testing area. The measured dielectric values were primarily used to scale the GPR images collected during the research.

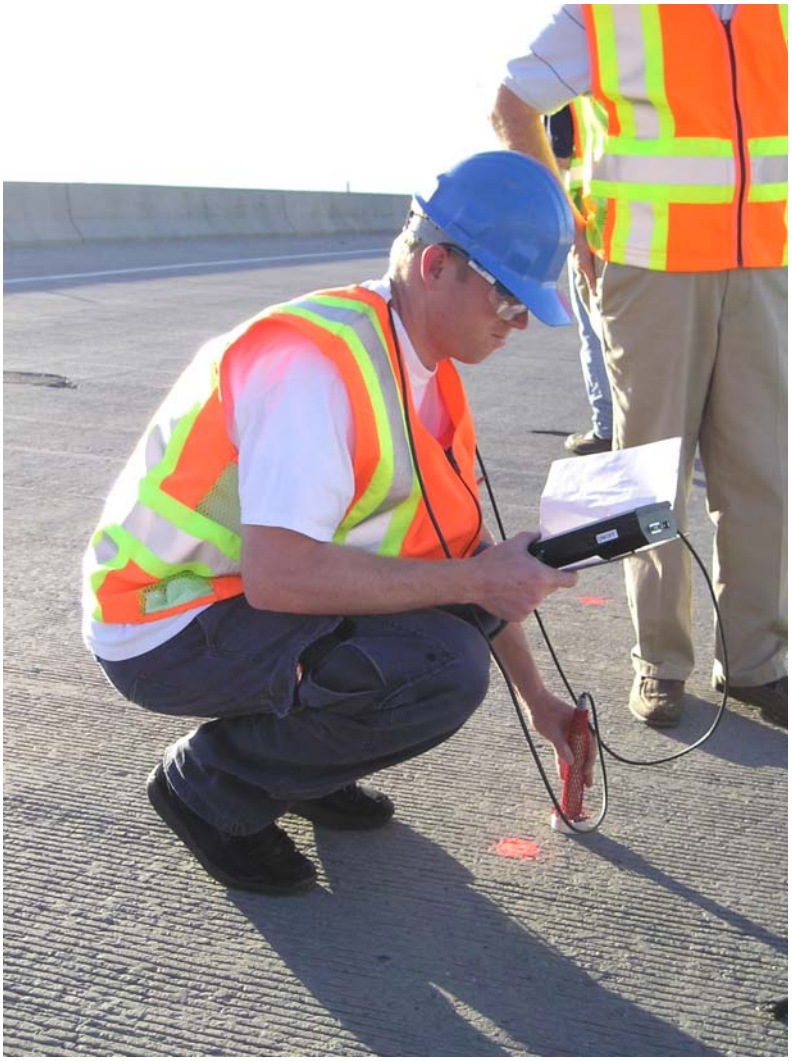

FIGURE 3.5 Measuring dielectric values.

3.6 GROUND-PENETRATING RADAR IMAGING

GPR imaging is a geophysical method that can be used to locate and map subsurface deck features such as reinforcing steel and delaminations. The apparatus emits electromagnetic radar waves into the bridge deck from an antenna placed on the deck surface (*12*, *19*, *20*). A GPR image is generated as waves are reflected back to the antenna after they come in contact with electrical interfaces between two media having different dielectric values. Damaged concrete causes an attenuation of the radar signal as the signal travels through the bridge deck and is reflected back from the damaged areas. A schematic of a typical GPR system is shown in Figure 3.6 (*11*).

Concrete bridge decks are ideal media for GPR surveys since concrete is primarily composed of sand and gravel, which both have low electrical conductivity values; generally, the depth of penetration decreases with increasing electrical conductivity (*21*). In this research, a longitudinal GPR profile of the deck testing area was generated. The linear imaging path followed one side of the testing area, near the station markers. Images of delaminations discovered by sounding methods were also collected. The GeoRadar GPR unit employed in this testing had a maximum operating frequency of 1.0 GHz and is shown in Figure 3.7.

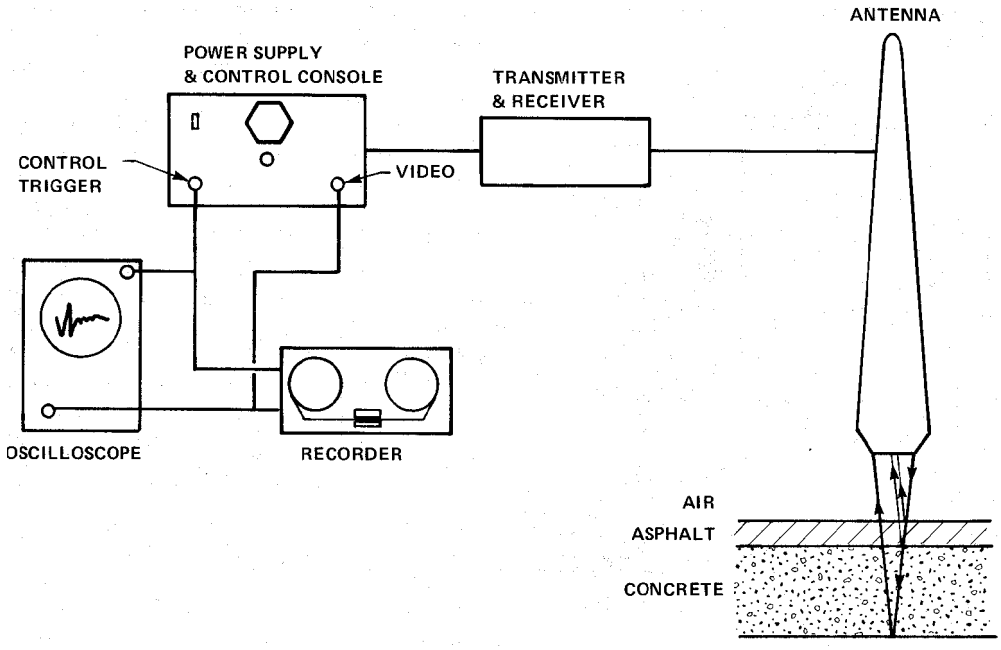

FIGURE 3.6 Schematic of a GPR system (*11*).

FIGURE 3.7 Ground-penetrating radar apparatus.

3.7 RESISTIVITY TESTING

Resistivity testing uses electrical resistance to evaluate the quality of reinforced concrete. Resistivity, which is the inverse of electrical conductivity, is a measure of the ability of a material to behave as an electrolyte, or to support corrosive electrical currents. Resistivity testing is different than the methods already discussed in that it measures the likelihood of the reinforcing steel to corrode rather than the amount of distress that has already occurred due to corrosion.

The ability of a material to resist ionic current flow depends upon both the porosity and water content of the medium. For example, very porous concrete with a high degree of saturation has a much lower resistivity than denser concrete with lower water contents; porous, saturated concrete permits soluble ions from deicing salts and other sources to more readily infiltrate the concrete. Consequently, the rate of corrosion dramatically increases as chloride ions migrate through the concrete to the reinforcing steel at faster rates and accumulate in higher concentrations within the concrete.

Even though numerous suggestions have been reported, a consensus has not yet been reached regarding appropriate resistivity threshold values for general

application. Tests have been performed to investigate the resistivity of concrete in various conditions. Moist concrete typically displays a resistivity of 3900 ohm-in., while oven-dried concrete exhibits a resistivity of 9400 Mohm-in. (*11*). Tests results indicate that corrosion is almost certain to occur when resistivity measurements are less than 2,000 ohm-in., probable when resistivity measurements are between 2,000 and 4,700 ohm-in., and unlikely when resistivity measurements are in excess of 4,700 ohm-in. (*11*). Other test results indicate that resistivity values between 2,000 and 3,900 ohm-in. are necessary to induce corrosion and that corrosion is unlikely to occur when resistivity levels exceed 7,900 ohm-in. (*11*).

The instruction manual for the resistivity meter used in this study provides a table, duplicated in Table 3.2, which correlates resistivity measurements to possible rates of reinforcement corrosion. While low levels of resistivity may occur due to the presence of diverse types of ions in the pore water, the suggested threshold values are based on the assumption that the decrease electrical resistance stems from the presence of sufficient chloride concentrations to induce corrosion of the reinforcing steel (*11*). Further research is needed to establish levels of resistivity that are reliably linked to corrosion potential and occurrence.

Another deficiency of the method is that the resistivity of concrete is most sensitive to near-surface conditions rather than to conditions in the vicinity of the reinforcement. Therefore, in this research, resistivity testing was used in conjunction with other testing methods (*11*).

The device utilized in this research to measure resistivity was an RM-8000 two-probe resistivity meter from NDT James Instruments, Inc. In the testing, two

TABLE 3.2 Resistivity Threshold Values for Corrosion Rates

Resistivity Levels (Ohm-in)	Possible Corrosion of Reinforcement
< 2,000	Very High
2000 to 4,000	High
4000 to 8,000	Moderate to Low
> 8,000	Insignificant

holes spaced 2 in. apart were drilled to a depth of 0.375 in. The holes were drilled with a hammer drill, cleaned with compressed air, and partially filled with a conductive gel as shown in Figures 3.8 through 3.10, respectively. Figure 3.11 shows the probe inserted into the holes for taking measurements. Two resistivity measurements were taken at each station using the same set of holes; the probe was simply rotated 180 degrees between readings.

FIGURE 3.8 Drilling holes in preparation for resistivity measurements.

FIGURE 3.9 Cleaning test holes with compressed air.

FIGURE 3.10 Placing conductive gel in test holes.

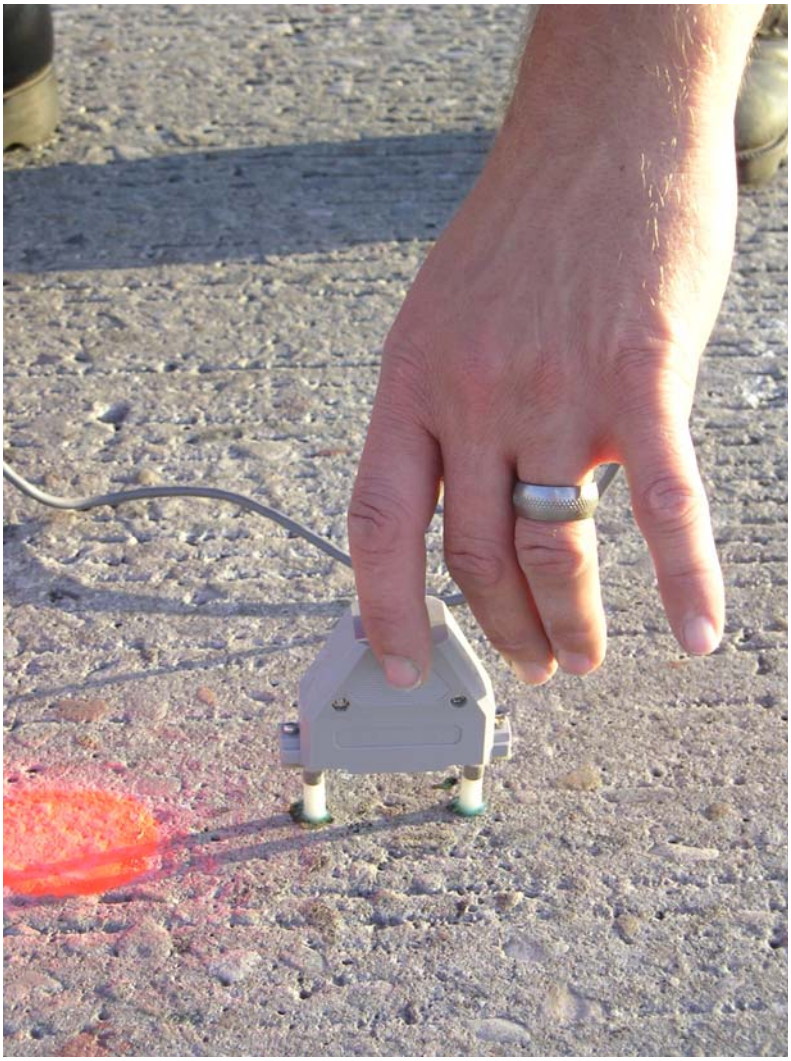

FIGURE 3.11 Using the two-probe resistivity meter.

3.8 HALF-CELL POTENTIAL TESTING

The severity of steel corrosion in each of the concrete decks was determined by measuring the electrical half-cell potential of the reinforcing steel at each station within the testing area. In the procedure employed in this research to obtain half-cell potential measurements, a Ferroscan instrument, shown in Figure 3.12, was used to determine the precise locations of steel reinforcement at both ends of the test section. After the reinforcement was located, a hammer drill, shown in Figure 3.13, was used to expose the steel. The depth of the reinforcement was verified using a digital micrometer as shown in Figure 3.14.

When the depth of the reinforcement was reached, drilling was terminated, and the hole was cleaned with compressed air. A hole was then drilled into the exposed steel for installation of a metal screw to which an electrical lead could be attached. Figure 3.15 shows the screw anchored in the reinforcing steel.

After screws were installed in the steel reinforcement at both ends of the test area, the electrical continuity of the steel mat between the screws was evaluated using the RM-8000 resistivity meter as shown in Figure 3.16. If the measured value of electrical resistance between the two points was less than 0.5 on the resistivity meter, electrical continuity between the anchor points was assumed to exist, and only one anchor point was used in the testing.

Half-cell potential measurements were then obtained using a copper-copper sulfate ($Cu\text{-}CuSO_4$) reference electrode (CSE), which was placed on the surface of the concrete where the steel reinforcement was located. The deck surface was sprayed with water, and a moist sponge was placed between the half-cell and the concrete to improve the electrical coupling between the deck and the instrument during the survey (*22*). The reference electrode was connected to the positive end of a high-input impedance voltmeter, and the negative end of the voltmeter was connected directly to the anchor point on the reinforcing steel being investigated.

In cases where electrical continuity did not exist, both anchor points were used for the half-cell potential survey. Because the exact location of the continuity break within a given test area could not be readily identified, the maximum distance from a given anchor point at which valid half-cell potential readings could be obtained was also unknown; therefore, readings were taken at every station from both anchor points. Figure 3.17 shows the data collection procedure. As with resistivity testing, two measurements were performed at each station. A schematic diagram of a half-cell apparatus is shown in Figure 3.18 (*22*).

FIGURE 3.12 Locating the steel reinforcement.

FIGURE 3.13 Drilling to expose the steel reinforcement.

FIGURE 3.14 Measuring the depth of steel reinforcement.

FIGURE 3.15 Screw installed in steel reinforcement.

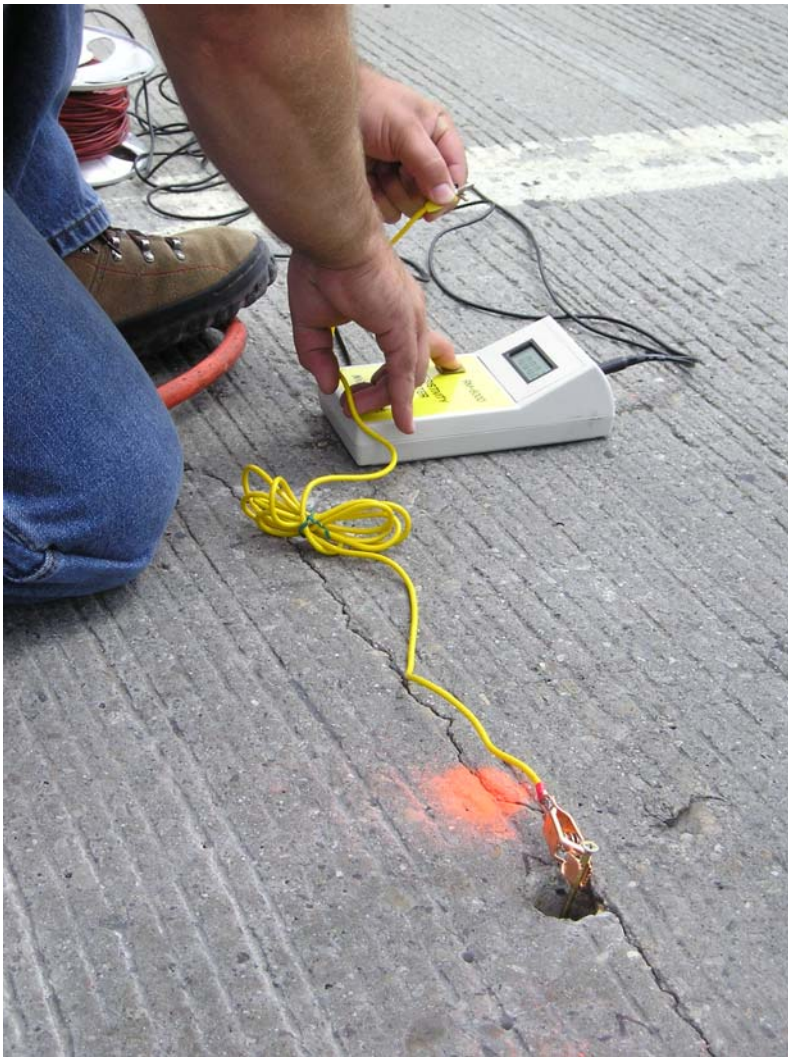

FIGURE 3.16 Testing electrical continuity of steel reinforcement.

FIGURE 3.17 Obtaining half-cell potential measurements.

According to American Society for Testing and Materials (ASTM) C 876, Standard Test Method for Half-Cell Potentials of Uncoated Reinforcing Steel in Concrete, potential measurements more negative than −0.35 V measured with a CSE indicate a probability greater than 90 percent that corrosion is occurring, potential measurements more positive than −0.20 V indicate a probability greater than 90 percent that corrosion is not occurring, and potential measurements between −0.20 and −0.35 V indicate that corrosion in that area is uncertain. While half-cell potential measurements indicate the probability of corrosion, they cannot be used to reliably estimate the rate of corrosion (*15, 24*).

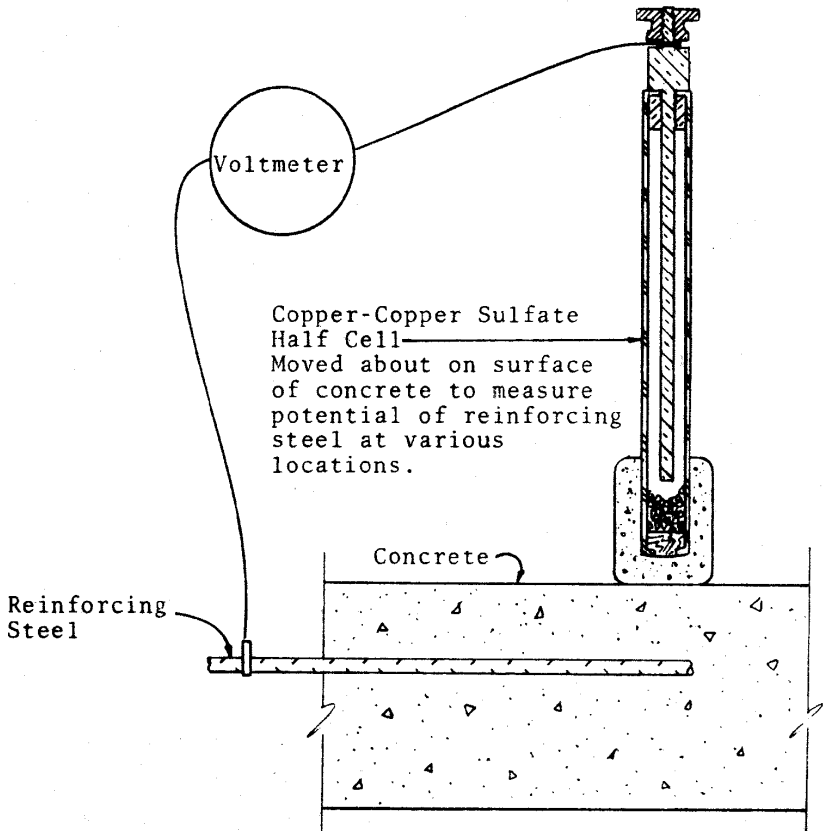

FIGURE 3.18 Diagram of a half-cell potentiometer (*23*).

Some research studies conflict with the potential threshold values designated by ASTM C 876 and suggest that the established values do not consider different conditions such as concrete moisture content, chloride content, temperature, carbonation, and cover thickness, which can alter the potential values associated with active corrosion of the reinforcing steel (*22*, *25*, *26*). The studies show that corrosion may begin at threshold values more positive than −0.20 V, as well as at values more negative than −0.35 V. The conclusion is that the threshold values of ASTM C 876 should only be used as guidelines since a precise delineation of steel from a passive to an active state cannot be made to encompass all conditions. In order to accurately formulate conclusions about corrosion of reinforcing steel, engineers and technical specialists should interpret potential measurements using supplementary data as appropriate (*23*). Nonetheless, an extensive area of potential measurements more

negative than −0.35 V implies a significant probability that corrosion is actively occurring in the affected area (*15*, *24*).

Two factors that affect half-cell potential measurements are concrete cover thickness and concrete resistivity. The relationship between concrete cover and the difference between the potential values of passive and corroding steel is inversely proportional. An increase in concrete cover decreases the difference between the potential values of passive steel and actively corroding steel and may cause the potential values to become nearly identical. Therefore, locating small corroding areas becomes extremely difficult with increasing cover depth, as illustrated in Figure 3.19 (*22*).

Half-cell potential measurements are also affected by the resistivity of the concrete, which in turn is affected by concrete pore water and ion concentrations in the pore solution. Researchers have shown that reduced electrical resistance of the concrete increases the current flow in the reference CSE, resulting in a lower half-cell potential reading that may suggest the presence of active corrosion (*22*).

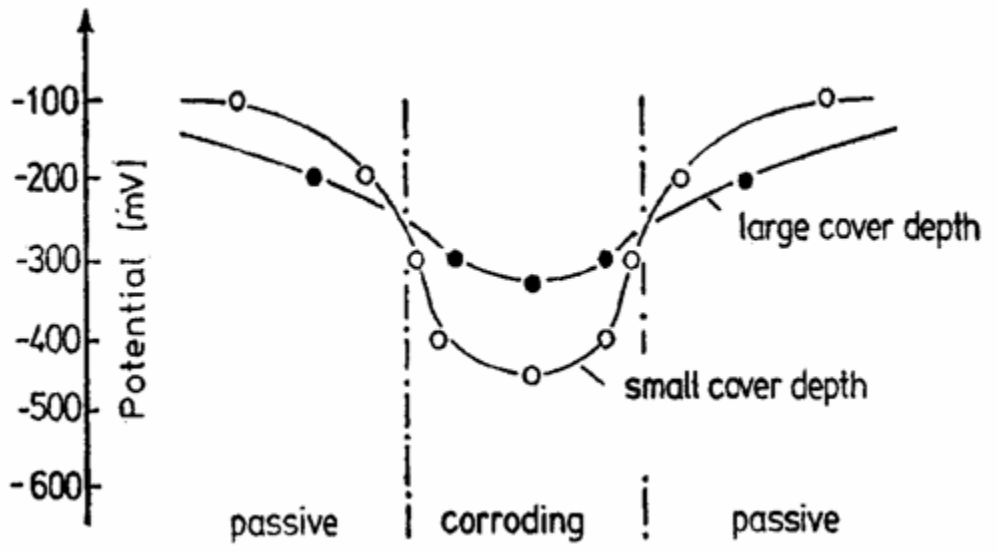

FIGURE 3.19 Plot of potential values with increasing cover depth (*22*).

3.9 CHLORIDE CONCENTRATION MEASUREMENTS

Chloride concentration testing can be used to identify areas of a bridge deck where chloride concentrations are high enough to initiate corrosion of the reinforcing steel. Of all the ions present in concrete, chlorides are of greatest concern. Not only do chloride ions react with iron in the steel reinforcement to produce rust, but the chlorides are released back into solution to react with more iron once rust is formed. Therefore, the chloride concentration does not markedly diminish with the formation of corrosion products. The recycling of chloride ions is the primary reason that steel reinforcement in chloride-contaminated concrete experiences comparatively rapid corrosion (*21*). The minimum chloride concentration necessary to initiate corrosion is generally accepted as 2 lbs of chloride per cubic yard of concrete in the vicinity of the reinforcing steel (*2*). According to some DOTs, full-deck replacement is required if more than 30 percent of the deck exceeds the threshold value (*2*).

To enhance testing efficiency in this research, the concrete removed to expose the reinforcing steel for half-cell potential testing was collected in approximately 1-in. depth increments for chloride concentration testing, as shown in Figure 3.20. As noted earlier, the concrete samples were obtained from the ends of the testing area on each deck, corresponding to stations 0 and 20.

During sample extractions, precautions were taken to ensure that contamination of progressively deeper concrete samples did not occur from inadvertent abrasion of upper sections of the test hole during drilling or from inadequate cleaning of the drill bit or test hole between lifts. In this study, both the test hole and drill bit were cleaned using pressurized air before beginning extraction of a new sample, and the drill operator was careful not to scrape the sides of the hole during further drilling. At each selected depth interval, the depth of the hole was measured using a digital micrometer.

The process of drilling, collecting the sample, and cleaning the hole was repeated for each depth increment until the depth of the reinforcement was reached. The pulverized concrete specimens were returned to the BYU Highway Materials Laboratory for chemical analyses.

FIGURE 3.20 Collecting pulverized concrete for chloride concentration analysis.

Chloride concentrations were determined using the soluble-chloride-ion method designated by ASTM C 1218, Standard Test Method for Water Soluble Chloride in Mortar and Concrete (*11, 27*). The method required that samples pass a No. 50 (0.0118-in.) screen, which was efficiently accomplished with the rotary-hammer method utilized for sample extraction (*11*). Samples were then boiled in water for 5 minutes and cooled for a period of 24 hours. The solution of soluble chloride ions was separated from the remaining pulverized sample by filtration and was subsequently treated with nitric acid and hydrogen peroxide. The chloride concentration of the solution was then measured using a laboratory chloride-ion-selective probe. The water-soluble test measures the quantity of free chloride ions and a portion of the chemically bound chloride ions.

3.10 SUMMARY

BYU researchers performed several non-destructive tests to assess the condition of each of the 12 concrete bridge decks evaluated in this study. The methods included visual inspection, sounding, dielectric measurements, GPR imaging, resistivity testing, half-cell potential testing, and chloride concentration measurements. Testing was only

performed on a representative 100 ft by 10 ft section of each bridge deck. Data resulting from the non-destructive testing procedures were compiled and evaluated in order to assess the condition of and recommend appropriate improvement strategies for each of the tested decks.

CHAPTER 4
TEST RESULTS

4.1 BRIDGE DECK CONDITION ASSESSMENT TESTING

Findings from the most recent bridge deck inspections conducted by UDOT, as well as a brief summary of past inspections, are reported in this chapter for each of the 12 concrete bridge decks evaluated in this research. Furthermore, the results of condition assessment testing conducted by BYU researchers are presented for each deck. The condition assessment testing included visual inspection, sounding, dielectric measurements, GPR imaging, resistivity testing, half-cell potential testing, and chloride concentration measurements. The bridge decks analyzed and compared in this study are presented in numerical order according to their identification number. Eleven of the bridges are owned by the State of Utah and routinely inspected by UDOT personnel. The twelfth bridge included in the study is owned by Spanish Fork City, although it is also regularly inspected by UDOT technicians.

4.2 BRIDGE DECK INSPECTIONS

Information summarized in this section is from the Structural Inventory and Appraisal Sheets and UDOT Bridge Inspection Reports associated with the tested decks. The data include evaluations of the bridge deck wearing surface, overall deck structure condition, and written notes describing the visual distresses observed on the deck at the time of inspection. The inspection process requires UDOT personnel conducting the inspections and writing the reports to assign ratings to the wearing surface condition and structural condition. The wearing surface condition rating includes general condition and top surface condition ratings, and the deck structure includes condition ratings for both the top and bottom surfaces of the deck and the deck overhangs. Condition rating for the bridge deck components are assigned as good (G), fair (F), or poor (P). The condition of

individual bridge deck components is considered in the process of assigning the bridge deck a numerical overall rating between 0 and 9, which is archived in the NBI database.

The individual component ratings and the overall ratings for the 12 decks tested in this research are presented in Table 4.1 together with the age of each bridge in 2005. Seven of the bridge decks are in good condition, four are in satisfactory condition, and one is in poor condition. Although a rating of 7 indicates that the deck is in good condition, some minor problems are likely present. Similarly, bridge decks with a numerical rating of 6 show some minor deterioration. A numerical rating of 4 indicates conditions such as advanced section loss, deterioration, and spalling or scouring (*7*).

Essentially, the overall deck ratings reflect the condition rating of the wearing surface and structural condition. However, some subjectivity was found in comparing bridges C-704 and C-637. Although both bridge decks were given the same overall condition rating of 6, the wearing surface and deck structure of C-704 were given ratings of fair and poor, while the components of C-637 were rated good and fair. Another concern is that ratings of 6 and 7 were assigned to bridge decks with similar conditions. For example, bridge decks C-460 and C-668 both have a good wearing surface and good to fair deck structural conditions but are assigned a rating of 7 and 6, respectively. These

TABLE 4.1 Deck Condition Rating

Bridge Deck Identification	Age (years)	Wearing Surface		Deck Structure			Rating (0 - 9)
		General	Top	Top	Bottom	Overhang	
C-460	17	G	G	G	-	F	7
C-493	30	F	F	-	P	P	4
C-635	23	G	G	G	F	G	7
C-637	19	G	G	G	F	F	6
C-654	26						7
C-668	19	G	G	-	-	F	6
C-693	22	G	G	F	F	F	7
C-702	20	G	P	P	F	F	6
C-704	20	F	P	P	F	F	6
C-769	14	G	G	G	G	G	7
F-477	17	G	G	G	G	G	7
F-595	9	G	G	-	G	G	7

observations highlight the need for more objective methods of assessing bridge deck condition.

During bridge inspections by UDOT personnel, observations regarding the condition of the decks were documented. The notes contain comments on the visual distresses and appearance of each deck, as well as the most recent MR&R actions in progress or completed. BMS software was implemented by UDOT in 1991, and as a result, only the most recent inspection notes, from 1991 to the present, are summarized in this report. Notes previous to 1991 were not available from UDOT. The earliest notes associated with inspections of bridges C-769 and F-595 were 1996 and 1998, respectively.

4.2.1 Inspection Notes for Bridge C-460

Bridge C-460 is a three-span bridge with a total span length of 227 ft. It is located on the Interstate 215 (I-215) corridor just south of the Interstate 80 (I-80) interchange and spans Indiana Avenue as shown in Figure 4.1. Information gathered from the UDOT inspection notes indicated that the deck had a series of full-depth transverse cracks in 1991. Stay-in-place (SIP) forms prevented inspection of the underside of the deck, but the overhangs

FIGURE 4.1 Map location of bridge C-460.

had light efflorescence. These conditions remained the same through 2003, with additional scaling of the deck occurring in 1998.

4.2.2 Inspection Notes for Bridge C-493

Bridge C-493, known as the Beck Street Bridge, is a nine-span bridge with a total span length of 812 ft. The bridge is located on Interstate 15 (I-15) corridor as shown in Figure 4.2. Deck conditions noted in 1991 included breaking up of the asphalt overlay, holes through the deck at the joints, longitudinal cracking on the underside of the deck with heavy efflorescence, some spalling at the joints that exposed corroded steel reinforcement, and longitudinal cracking caused by corrosion of the steel girders.

The condition of the deck continued to gradually worsen through 2004. Further deterioration included failed expansion joints that allowed water to flow freely through the deck onto the substructure, random vertical cracking on the parapets with heavy scaling and some spalling to the depth of the reinforcement, some stalagmites, and delaminations.

FIGURE 4.2 Map location of bridge C-493.

4.2.3 Inspection Notes for Bridge C-635

Bridge C-635 is a two-span bridge with a total span length of 280 ft. The bridge spans Bangerter Highway and is a collector for eastbound traffic on I-80 as shown in Figure 4.3. Existing conditions in 1991 included a series of full-depth transverse cracks and light efflorescence on the underside of the deck, which remained the same through 2005. An entry in 2003 clarified that the transverse cracking was located in the southern portion of the bridge deck only and that no cracking was present in the northern span.

FIGURE 4.3 Map location of bridge C-635.

4.2.4 Inspection Notes for Bridge C-637

Bridge C-637 is a two-span bridge with a total span length of 842 ft over I-80 and serves as a collector for eastbound traffic on I-80 as shown in Figure 4.4. The UDOT inspector noted in 1991 that the underside of the deck had a series of transverse cracks with light efflorescence in the negative moment areas. In 1995 inspectors noted that the faces of the parapets were scaling and the concrete along the north expansion joint was disintegrating. In 1997, the parapets were sealed and new expansion joints were installed, but the joints had to be replaced again in 2001. Also in 2001, a new polymer wearing course was placed on the entire deck surface. However, the cracking and efflorescence on the underside of the deck remained. Several potholes developed in 2002 and 2004, and, although they were filled, they need to be repaired again.

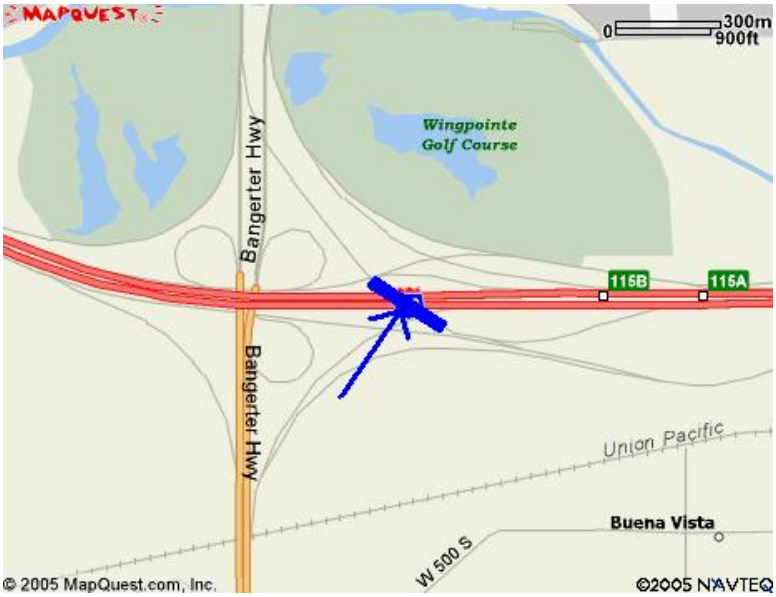

FIGURE 4.4 Map location of bridge C-637.

4.2.5 Inspection Notes for Bridge C-654

Bridge C-654 is a three-span bridge with a total span length of 101 ft over railroad tracks near State Route 6 (SR-6) in Spanish Fork, Utah, as shown in Figure 4.5. Although the bridge is routinely inspected by UDOT personnel, the inspection notes were given to Spanish Fork City and were not available for review in this research.

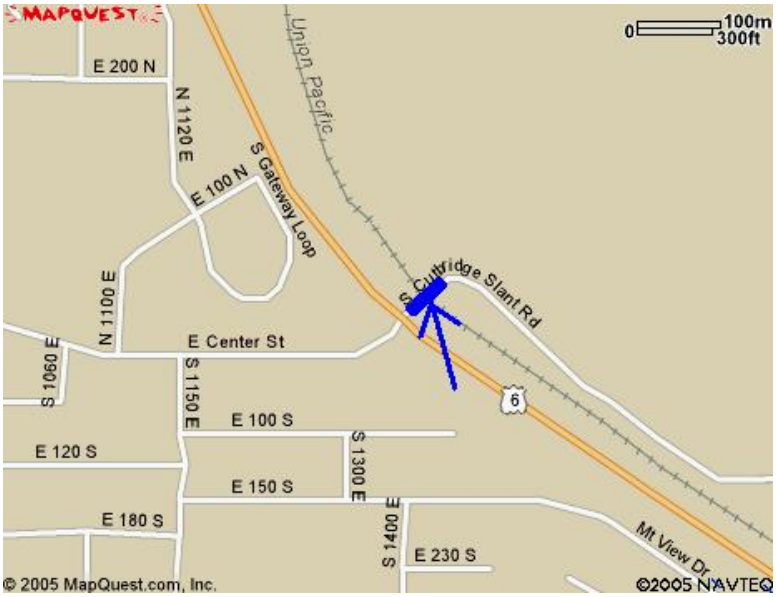

FIGURE 4.5 Map location of bridge C-654.

4.2.6 Inspection Notes for Bridge C-668

Bridge C-668 is a two-span bridge on Bangerter Highway. The bridge has a total span length of 236 ft over railroad tracks as shown in Figure 4.6. The only existing condition noted in 1991 was transverse cracking on the underside of the deck overhangs.

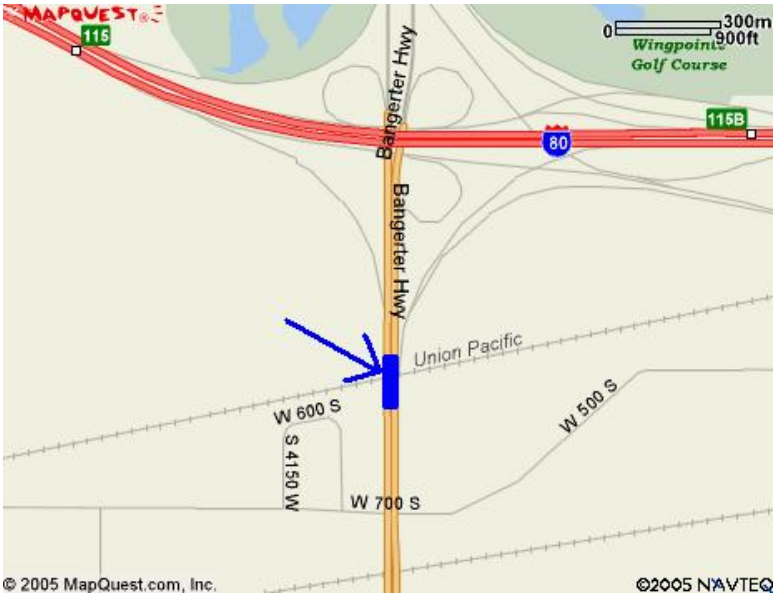

FIGURE 4.6 Map location of bridge C-668.

Efflorescence began to appear in 1995, and in 1996 the SIP forms had developed rust, which worsened through the year 2000. A regular series of full-depth transverse cracks had developed by 2002. The thin overlay installed before the 2002 inspection did not prevent infiltration of water and had deteriorated in four areas of the deck by 2005.

4.2.7 Inspection Notes for Bridge C-693

Bridge C-693 is a two-span bridge with a total span length of 196 ft on the I-215 corridor spanning West North Temple as shown in Figure 4.7. The condition assessment conducted in 1991 reported transverse cracking with efflorescence on the underside of the deck at negative moment regions; in 1995, the spacing of the transverse cracks was noted to be between 2 ft and 3 ft. In 1996, longitudinal cracking was evident at the abutments. By 1998, longitudinal cracking was also present on the underside of the deck. All cracking appeared to be full-depth, with flaking of the concrete on the top side of the deck and light to moderate efflorescence on the underside of the deck. In 2003, full-depth diagonal and vertical cracking with efflorescence had developed on the deck overhangs.

FIGURE 4.7 Map location of bridge C-693.

4.2.8 Inspection Notes for Bridge C-702

Bridge C-702 is a two-span bridge with a total span length of 331 ft over I-80. The bridge serves as a collector for northbound traffic on I-215, as shown in Figure 4.8. As of 1991, the underside of the deck had experienced extensive full-depth transverse cracking, some diagonal cracking in the corners, and light to moderate efflorescence. The parapets had also experienced some scaling. These conditions remained the same until 2000, when the efflorescence on the bottom of the deck was reported to be more severe. In addition, potholes had begun forming on the top surface. Several potholes had fully developed by 2003 and 2005, as well as 0.25-in. wide cracking on the top surface with efflorescence on the bottom.

FIGURE 4.8 Map location of bridge C-702.

4.2.9 Inspection Notes for Bridge C-704

Bridge C-704 is a two-span bridge with a total span length of 530 ft over an I-80 collector and is part of the I-215 corridor as shown in Figure 4.9. Existing conditions in 1991 included transverse cracks spaced 2 ft to 3 ft apart on the bottom of the deck with significant amounts of moderate to heavy efflorescence, loose expansion joints that allowed water to leak directly onto bearing plates to form rust, and some holes that were drilled in the deck for drainage but were not lined with any type of protective coating. In 2003 additional transverse cracking was observed on the top surface of the deck with large areas of spalling and exposed reinforcement. An estimated 10 percent of the deck area exhibited delaminations and spalling.

FIGURE 4.9 Map location of bridge C-704.

4.2.10 Inspection Notes for Bridge C-769

Bridge C-769 is a five-span bridge that is part of SR-201. The bridge has a total span length of 769 ft over the I-80 corridor and acts as a collector for westbound traffic on I-80 as shown in Figure 4.10. The earliest inspections notes available for this bridge were from 1996. Conditions in 1996 included transverse cracking with efflorescence on the bottom of the deck, spalling with exposed reinforcement at the southwest and northwest

FIGURE 4.10 Map location of bridge C-769.

corners of the underside of the deck, and several potholes on the top surface of the deck. In 2000 the parapet on the east side had areas of collision damage.

4.2.11 Inspection Notes for Bridge F-477

Bridge F-477 is a single-span bridge with a total span length of 144 ft over 1700 South and is part of the I-215 corridor just north of SR-201, as shown in Figure 4.11. As of 1991, the bridge had several full-depth transverse and diagonal cracks, as well as diagonal cracks in the corners of each individual bay between beams. Light efflorescence on the underside of the deck was also observed. The conditions remained the same through 2003, when the parapets were reported to have minor cracking, light efflorescence, and scaling.

FIGURE 4.11 Map location of bridge F-477.

4.2.12 Inspection Notes for Bridge F-595

Bridge F-595 is a three-span bridge with a total span length of 235 ft over railroad tracks. The bridge is part of SR-202 near I-80, as shown in Figure 4.12. The earliest inspection notes available for this bridge deck are from 1998 and indicate that an epoxy-based

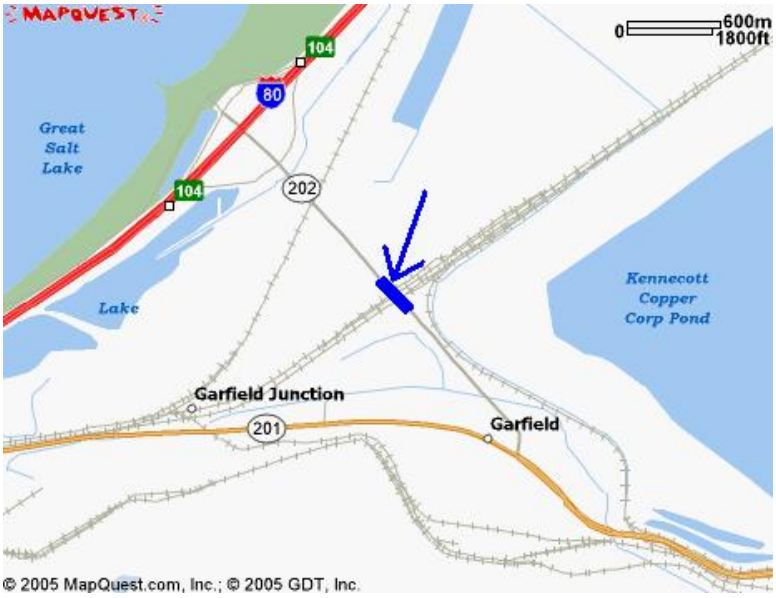

FIGURE 4.12 Map location of bridge F-595.

overlay had been placed on the deck surface and was still in good condition. By 2000, an asphalt overlay had been placed on the deck. The wearing surface was reported to be in good condition in 2002, with no moisture penetrating through the deck. In 2004, a polymer overlay had replaced the asphalt.

4.2.13 Summary of Inspection Notes

The most common distress noted in all bridge decks is full-depth transverse cracking with efflorescence. Exposed reinforcement was observed in three of the bridge decks; spalling, scaling, and potholing of the concrete deck structure were noticed in four bridge decks; delaminations were detected in two bridge decks; and rust stains were exhibited on the surface of one bridge deck. These distresses reflect the current conditions of the deck and generally verify the condition rating assigned to each bridge deck by UDOT inspectors.

4.3 DECK TEST SECTION

Testing of the entire bridge deck was not feasible and therefore outside the scope of this research. Nonetheless, the location of the testing area on each bridge deck was located in order to best represent the overall condition of the deck. A summary of the length, width, area, and percentage of the deck that was tested is shown in Table 4.2 for all 12 decks. The specific location of the testing area on each bridge is represented by a rectangular outline within a lane of traffic, as shown in Figures 4.13 through 4.24. The solid gray line designates the center line, the dark solid line represents the outer lane marking, and the double line indicates the location of a parapet. Due to the length of some bridges, only a portion of the bridge is shown. Bridge dimensions were obtained from the Structural Inventory and Appraisal Sheets provided by UDOT. Although specified dimensions are accurate, the figures are not drawn to scale.

The location of the testing area was different on each bridge deck. The testing area for bridge C-460 was located 104.7 ft from the northern edge of the bridge deck. Unfortunately no reference point was selected for bridges C-493, C-635, or C-637. The testing area for bridge C-654 was the entire traffic lane on the north side of the bridge deck. For bridge C-668, the test area was located 20 ft from the joint between

TABLE 4.2 Percentage of Deck Area Tested

Bridge Deck Identification	Length (ft)	Width (ft)	Area (ft^2)	Percent of Deck Tested (%)
C-460	227	156	35381	2.8
C-493	812	84	68200	1.5
C-635	260	59	15260	6.6
C-637	842	39	32592	3.1
C-654	101	31	3131	31.9
C-668	236	70	16485	6.1
C-693	196	179	35086	2.9
C-702	331	27	8906	11.2
C-704	530	132	70056	1.4
C-769	769	28	21446	4.7
F-477	144	179	25753	3.9
F-595	235	73	17032	5.9

the southern approach slab and the deck and offset 8 ft from the barrier. The testing area for bridge C-693 was located 40.7 ft from the northern edge of the bridge deck. The test area for bridge C-702 was located 4 ft south of the sixth barrier joint on the west side of the bridge. For bridge C-704, the testing area was located 20.2 ft from the first diagonal joint following the southernmost edge of the bridge deck and the end joint of the entry slab. The testing area for bridge C-769 was located 292.5 ft north of the joint between the deck and approach slab. The testing area for bridge F-477 was located 43.6 feet from the northern edge of the bridge deck. For bridge F-595, the testing area was located 27 ft from the joint between the northern approach slab and the deck and offset 11 ft from the barrier.

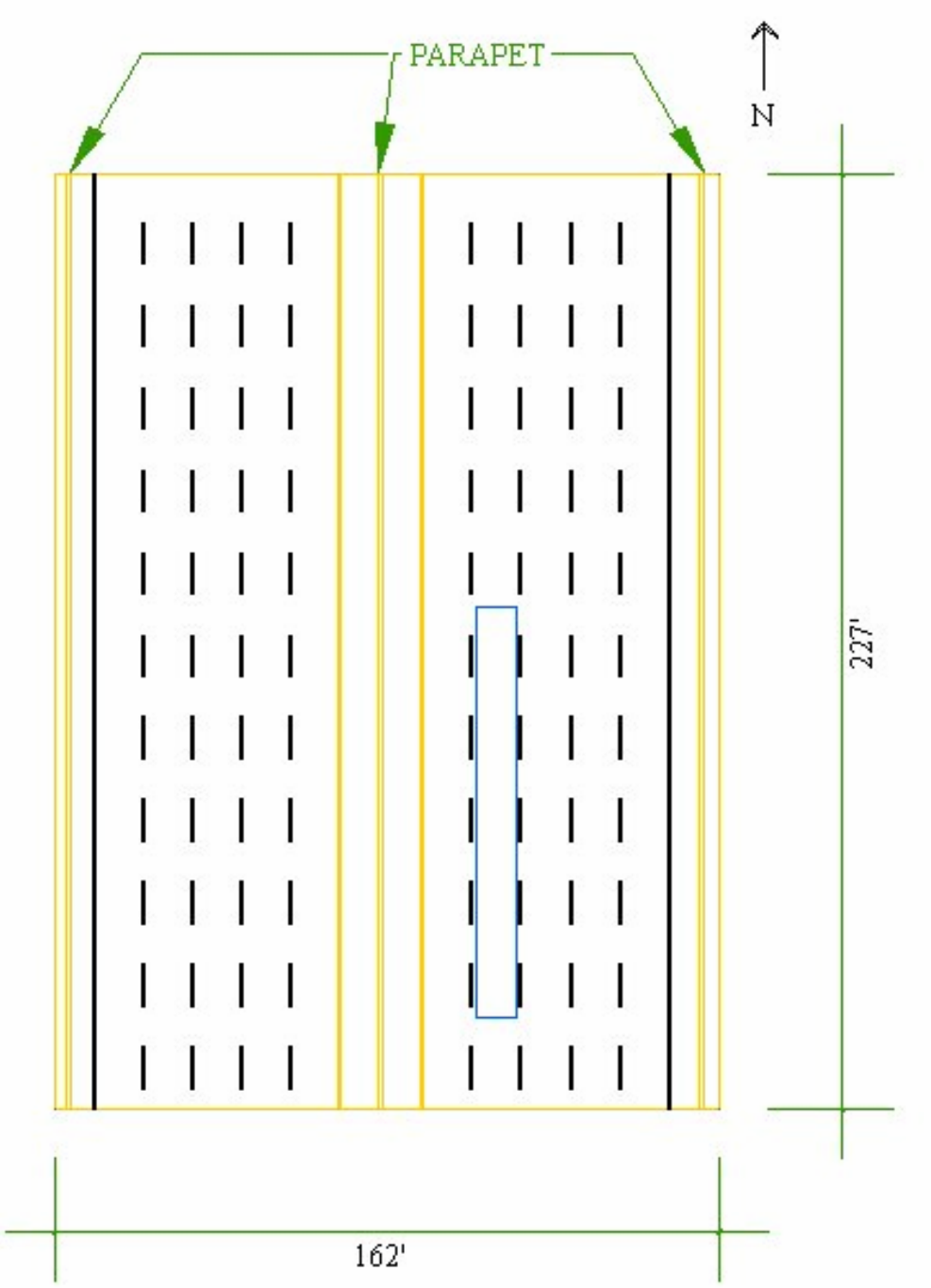

FIGURE 4.13 Testing area on bridge C-460.

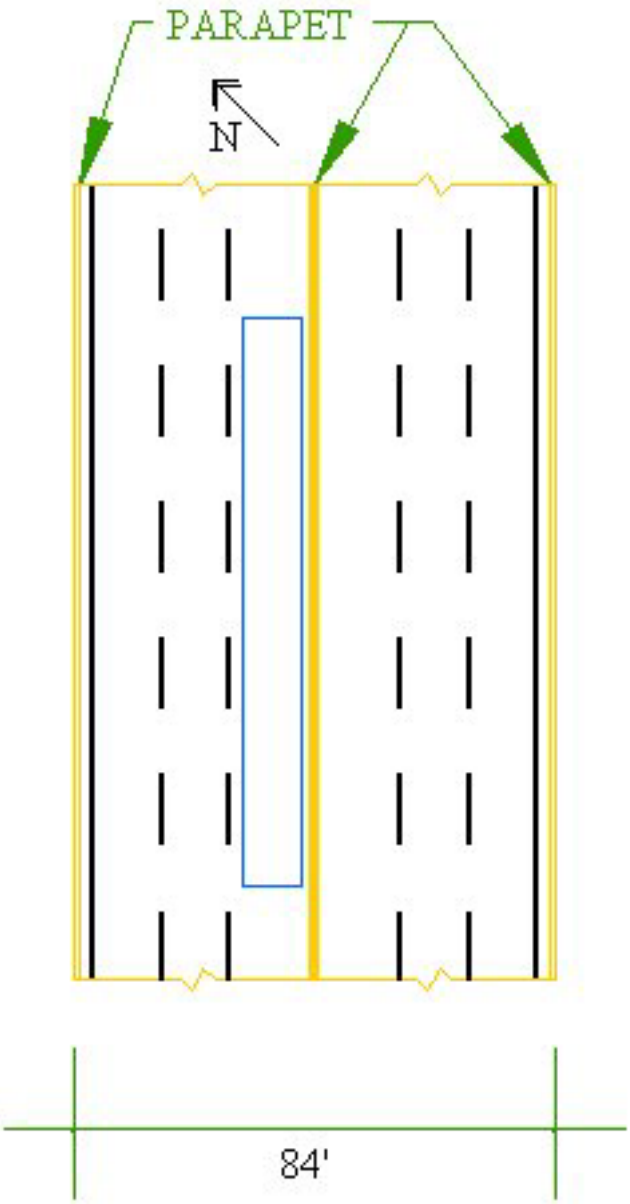

FIGURE 4.14 Testing area on bridge C-493.

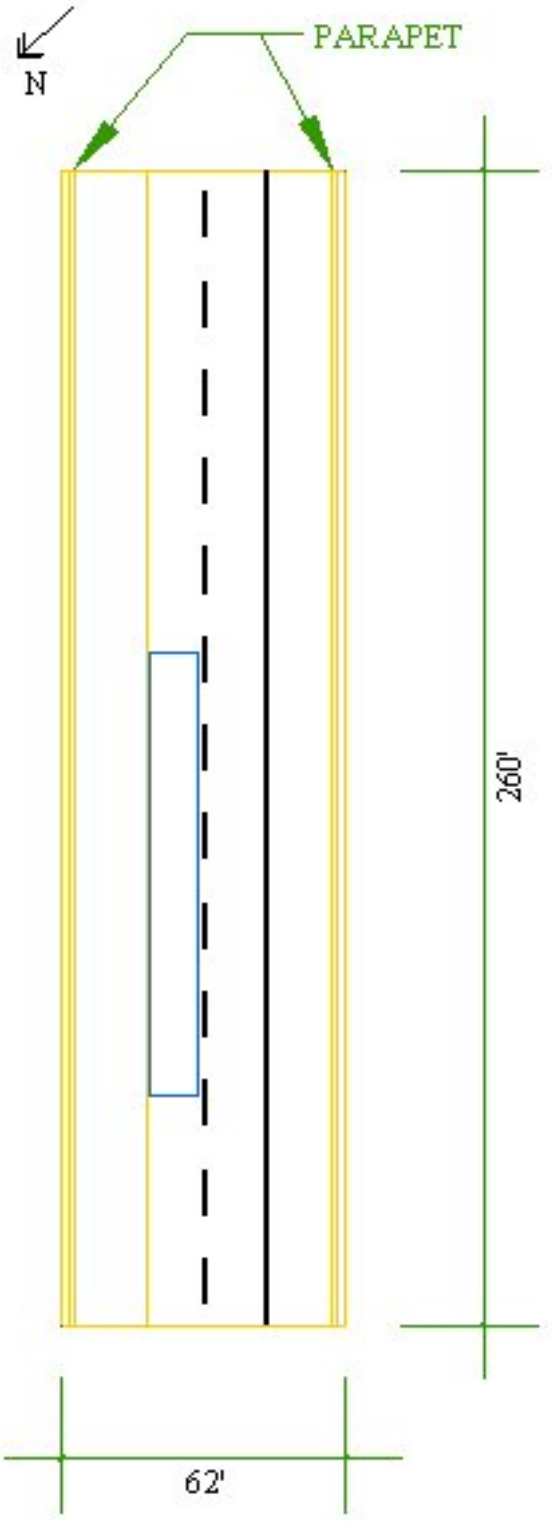

FIGURE 4.15 Testing area on bridge C-635.

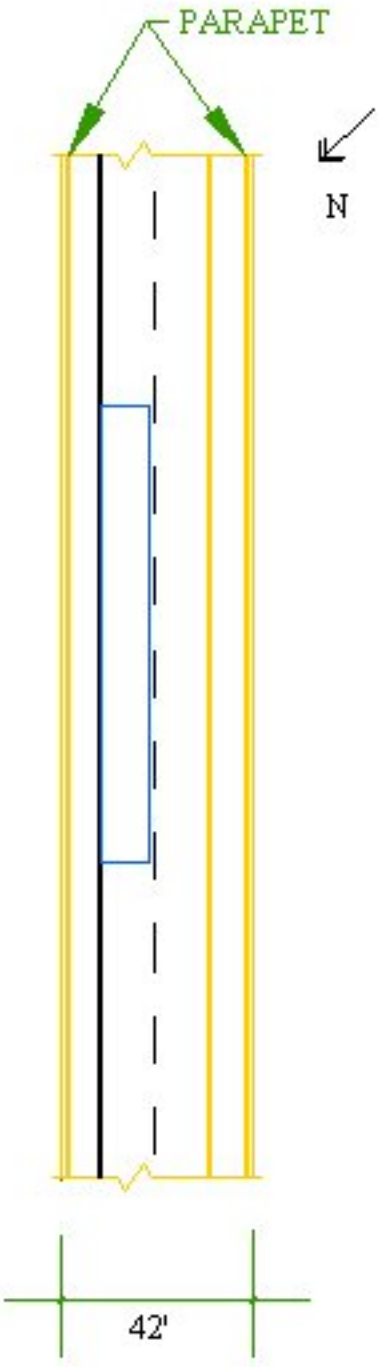

FIGURE 4.16 Testing area on bridge C-637.

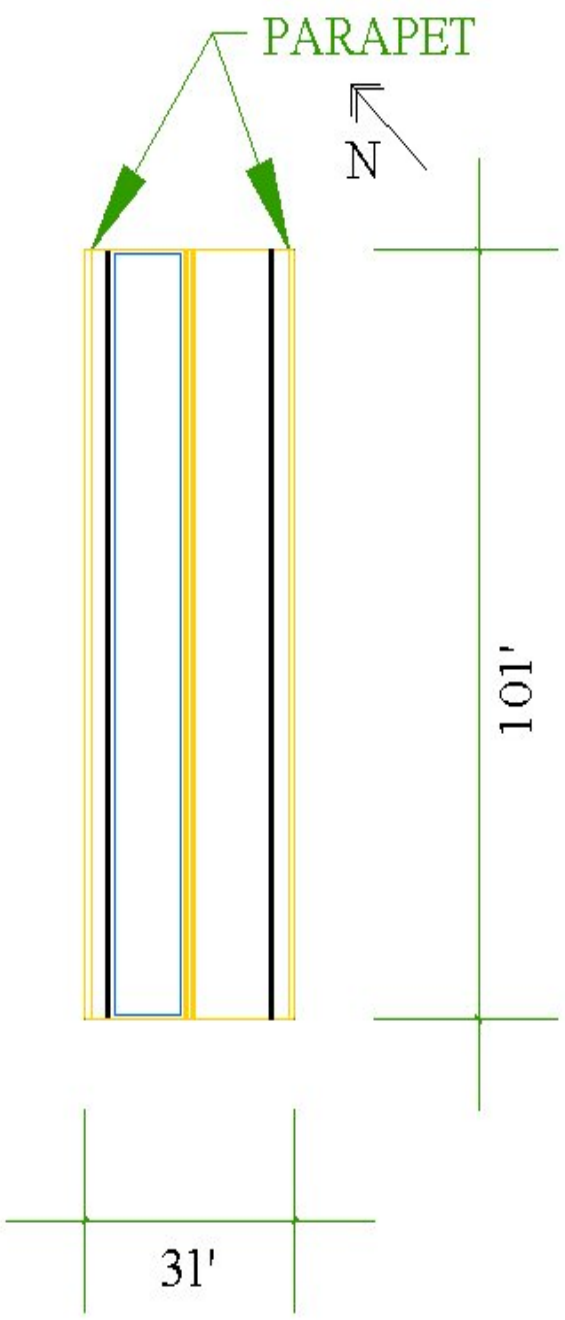

FIGURE 4.17 Testing area on bridge C-654.

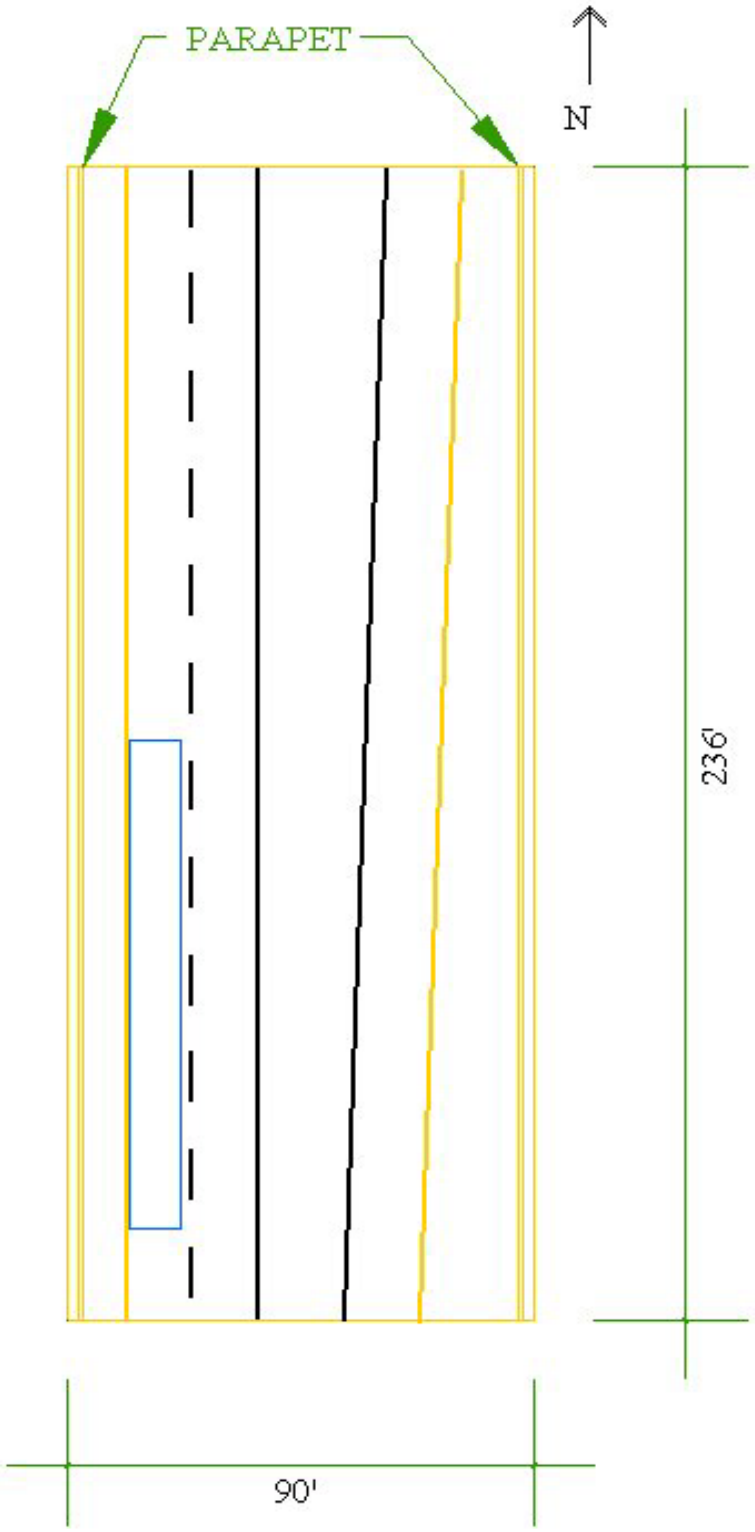

FIGURE 4.18 Testing area on bridge C-668.

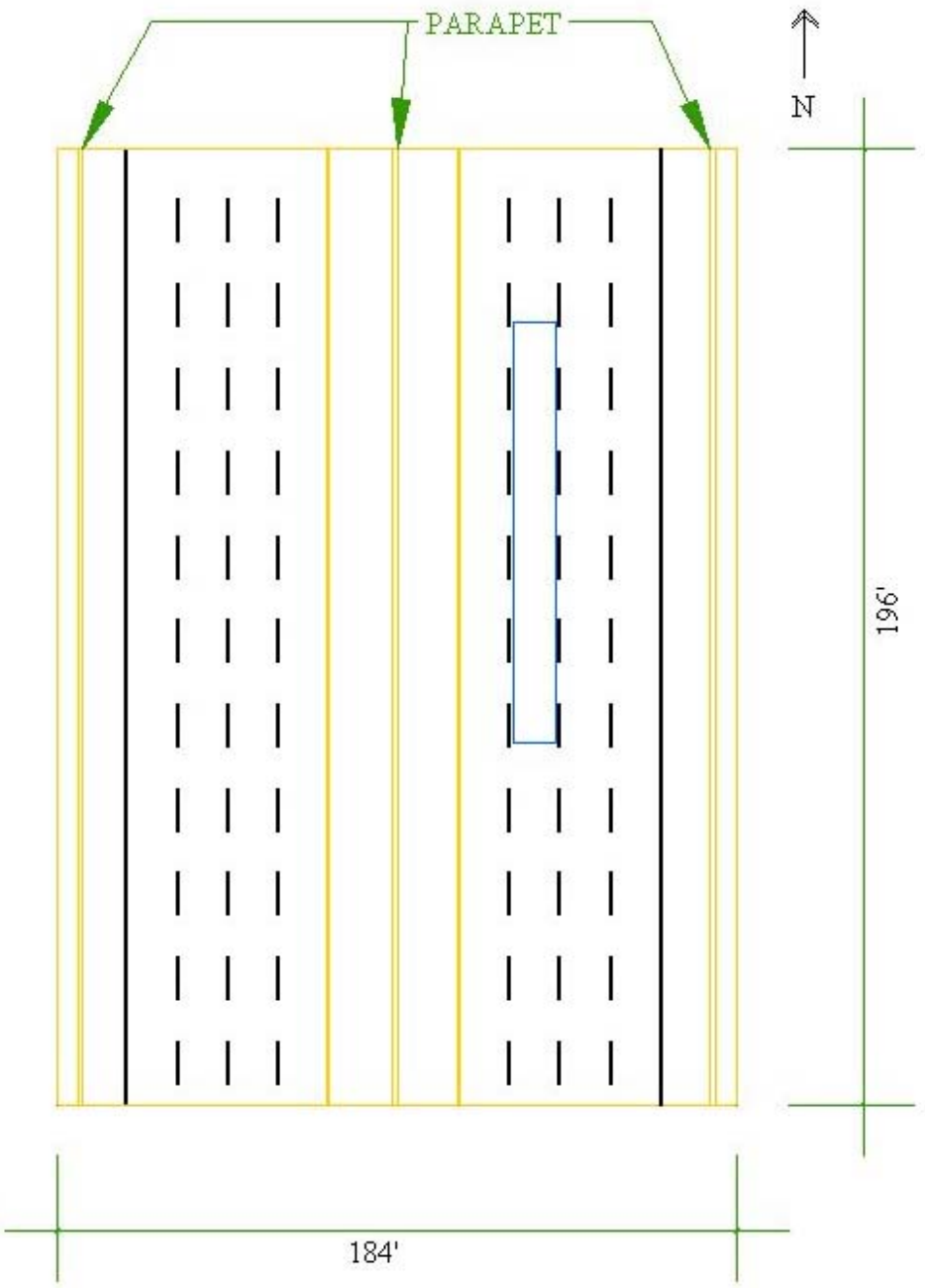

FIGURE 4.19 Testing area on bridge C-693.

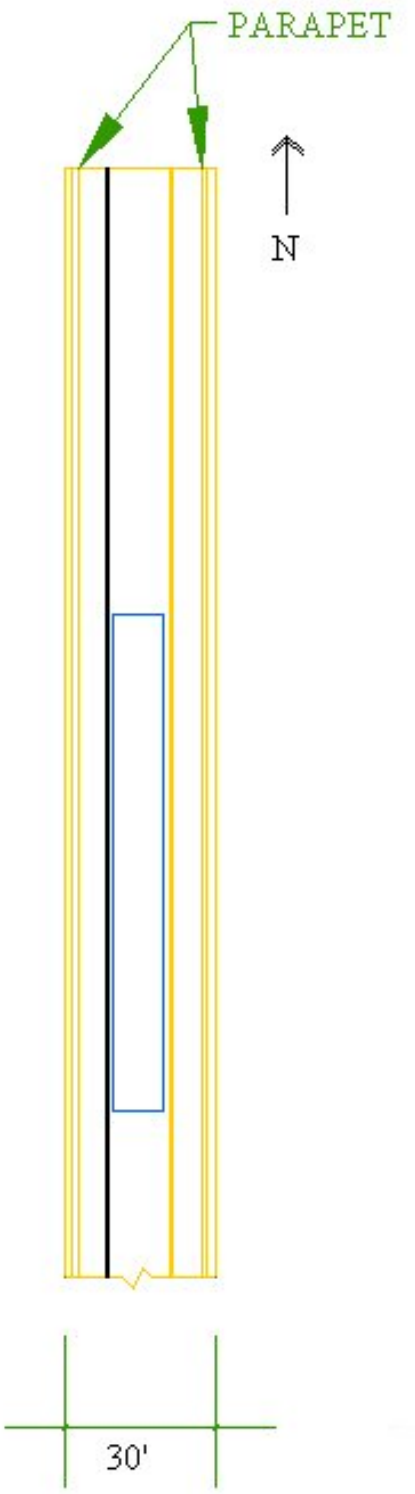

FIGURE 4.20 Testing area on bridge C-702.

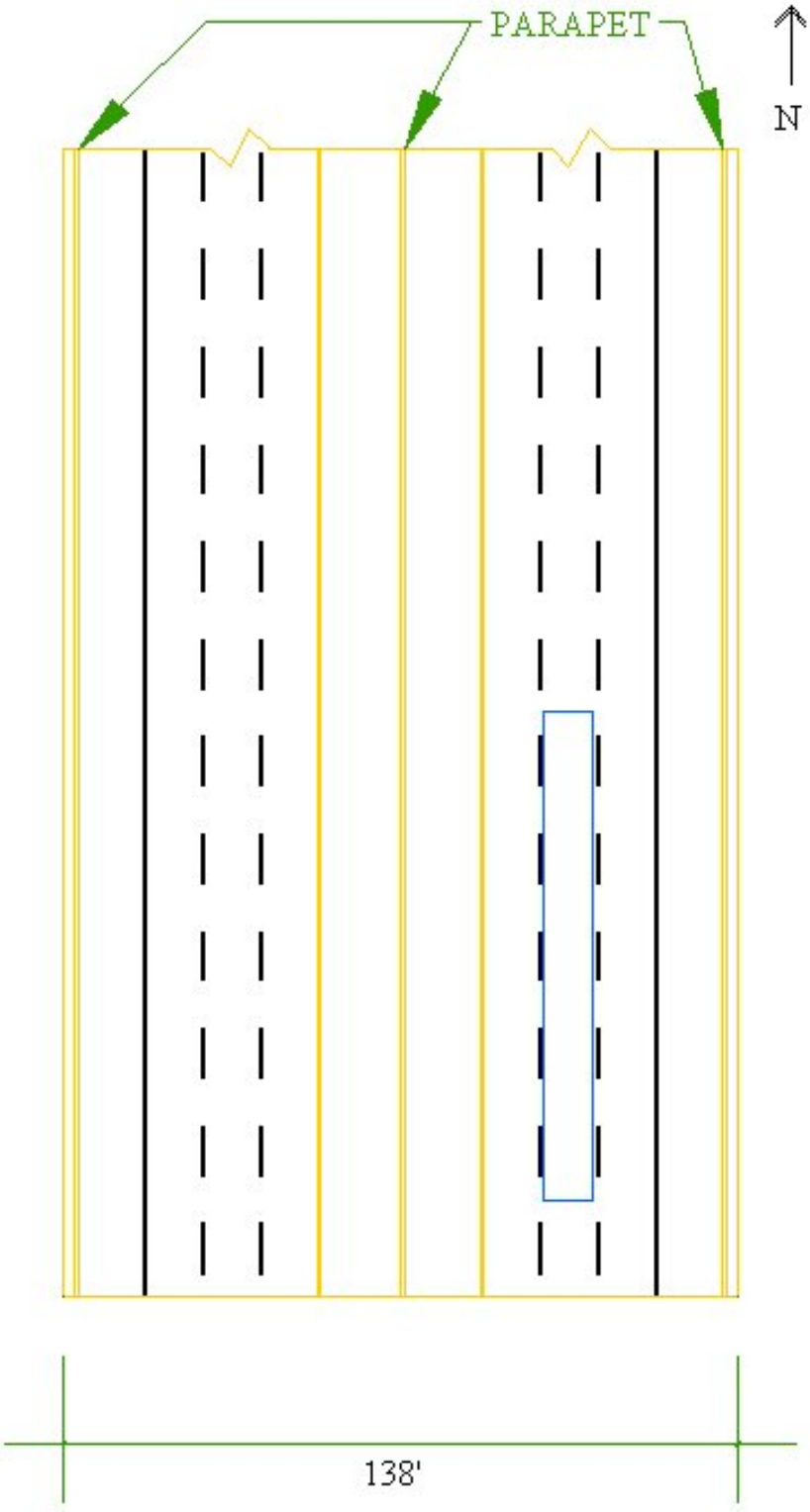

FIGURE 4.21 Testing area on bridge C-704.

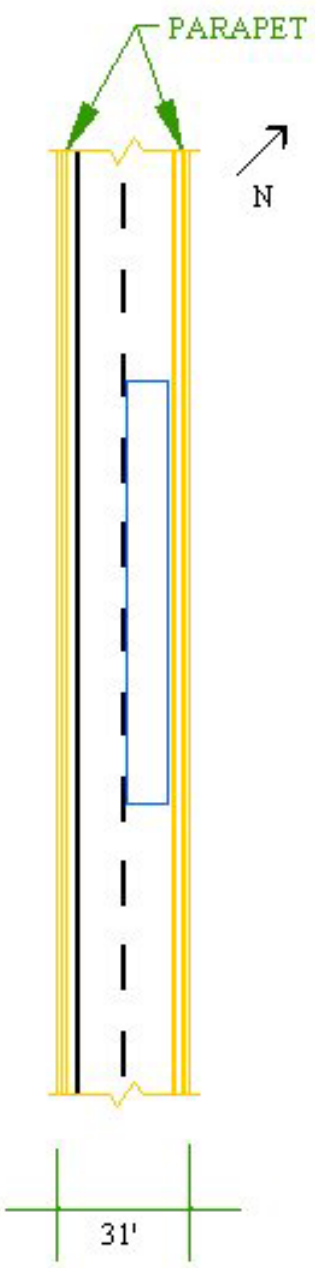

FIGURE 4.22 Testing area on bridge C-769.

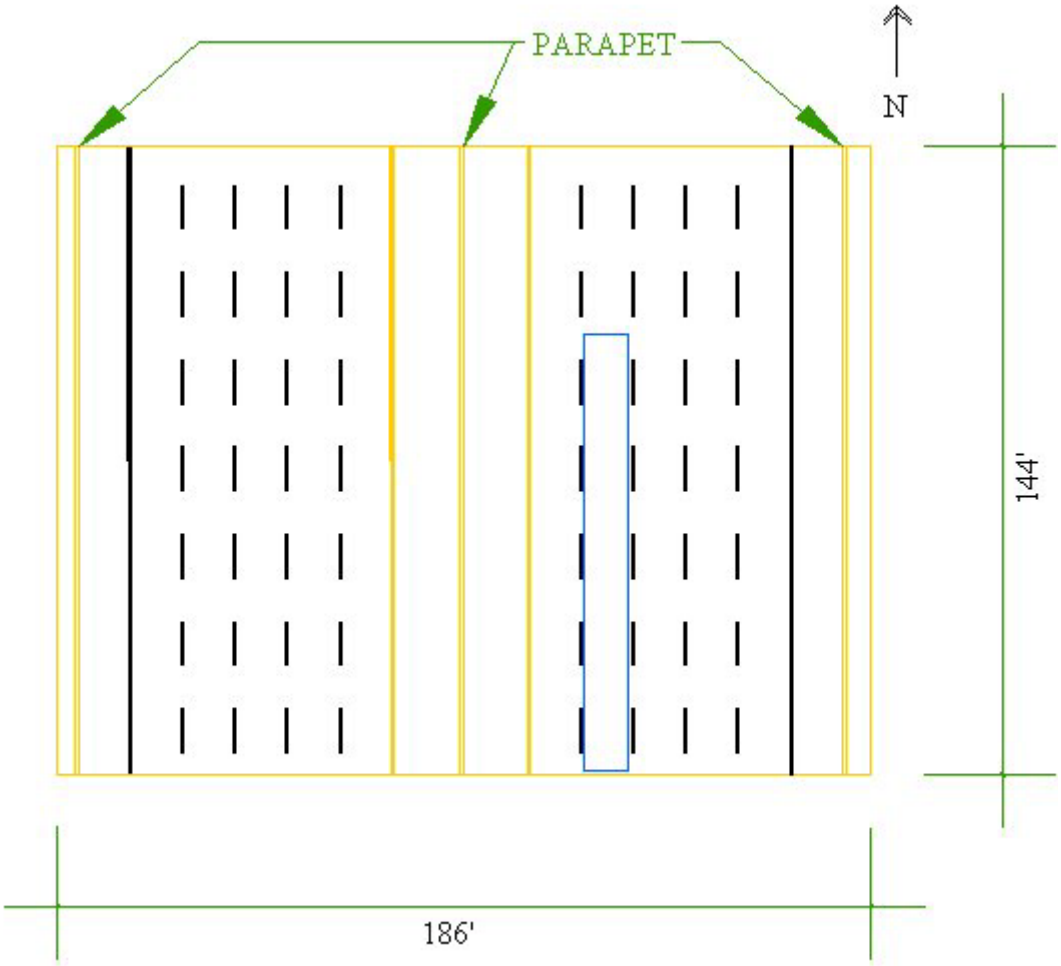

FIGURE 4.23 Testing area on bridge F-477.

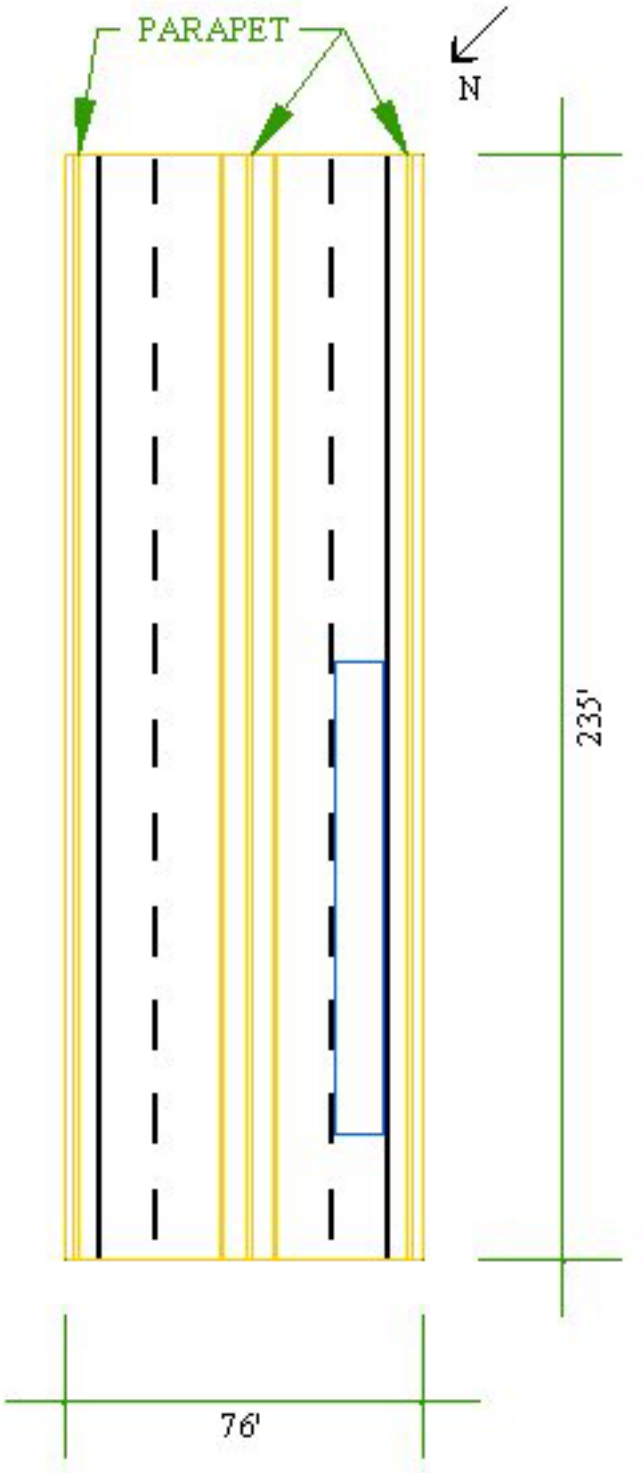

FIGURE 4.24 Testing area on bridge F-595.

4.4 VISUAL INSPECTIONS

As part of the visual inspections conducted in this research project, distress surveys were compiled, and photographs of most of the bridge decks were taken. Distress types and locations for the surveyed sections were documented on distress survey worksheets, which are presented in Figures 4.25 through 4.36. The worksheets divide the 100-ft by 10-ft testing area into two 50-ft by 10-ft sections with stationing at 5-ft increments numbered from 0 to 10 and 10 to 20 on the left side of the two sections. All distress measurements were taken within the testing area on the top surface of each deck. Crack widths are reported in inches, and the locations of delaminations, potholes, and other defects are labeled on the distress surveys. The average crack density, crack severity, and pothole density were computed using the data collected during the distress survey. Photographs taken to document bridge deck condition were not limited to just the testing area, however, but were representative of the entire bridge deck.

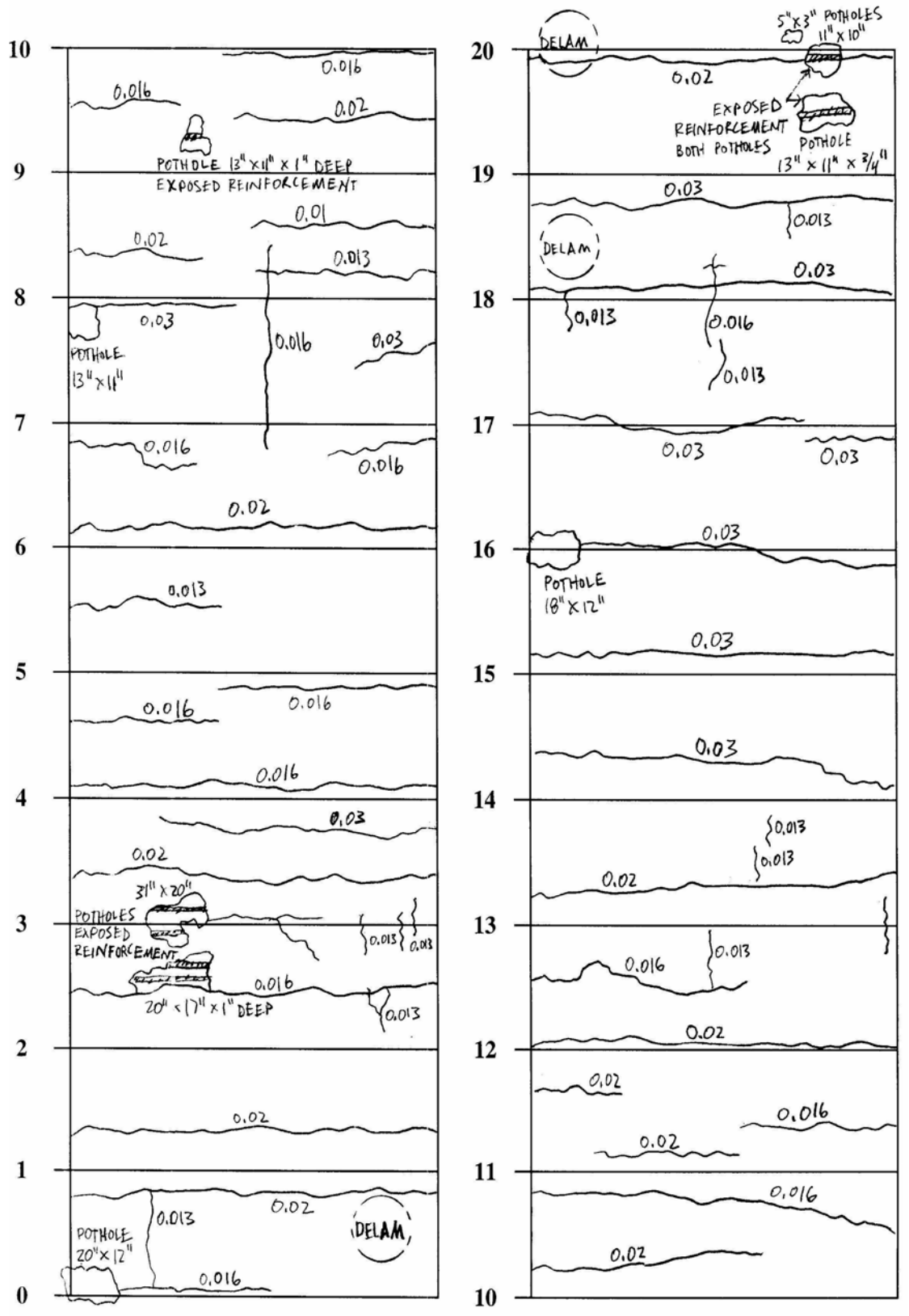

FIGURE 4.25 Distress survey of bridge C-460.

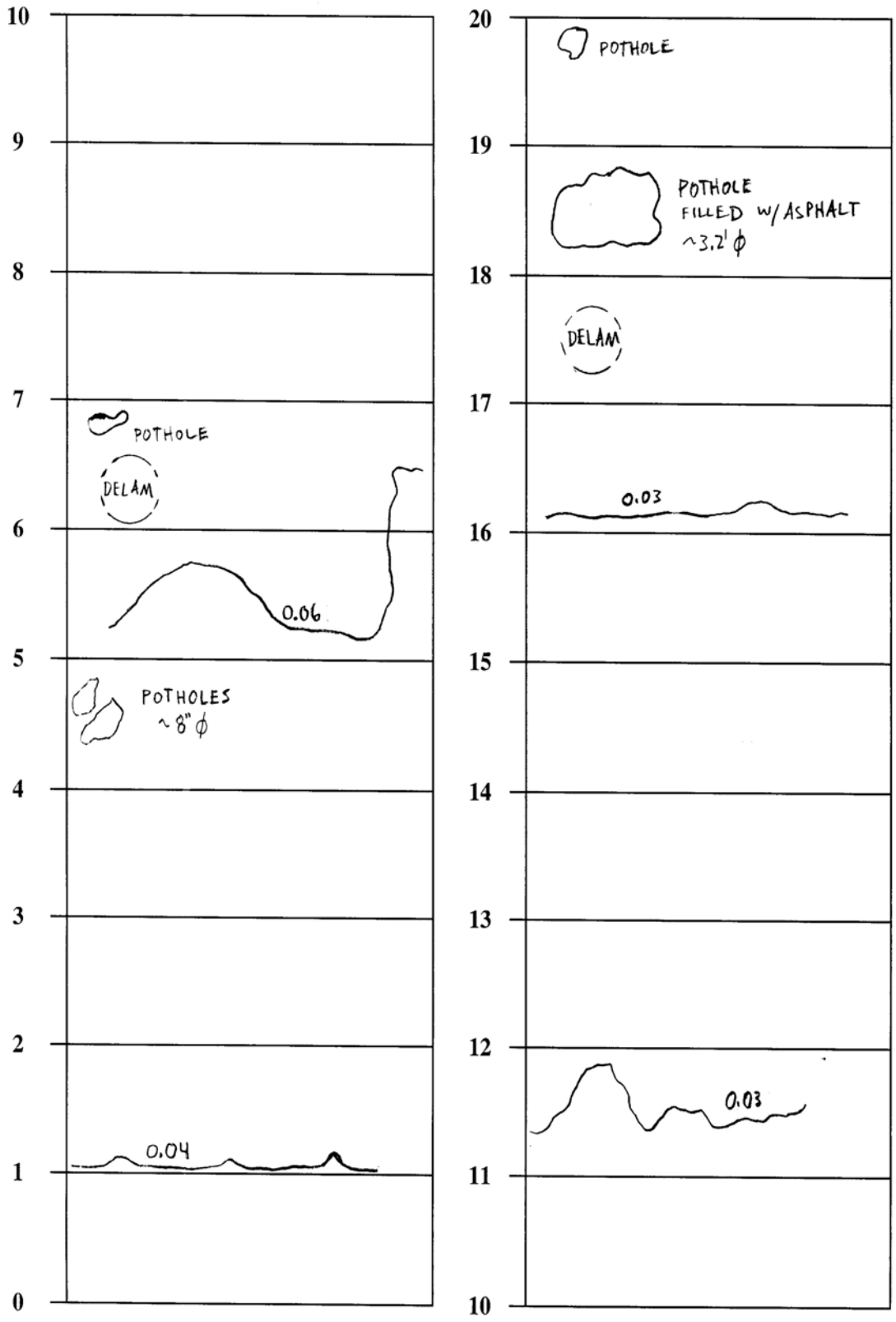

FIGURE 4.26 Distress survey of bridge C-493.

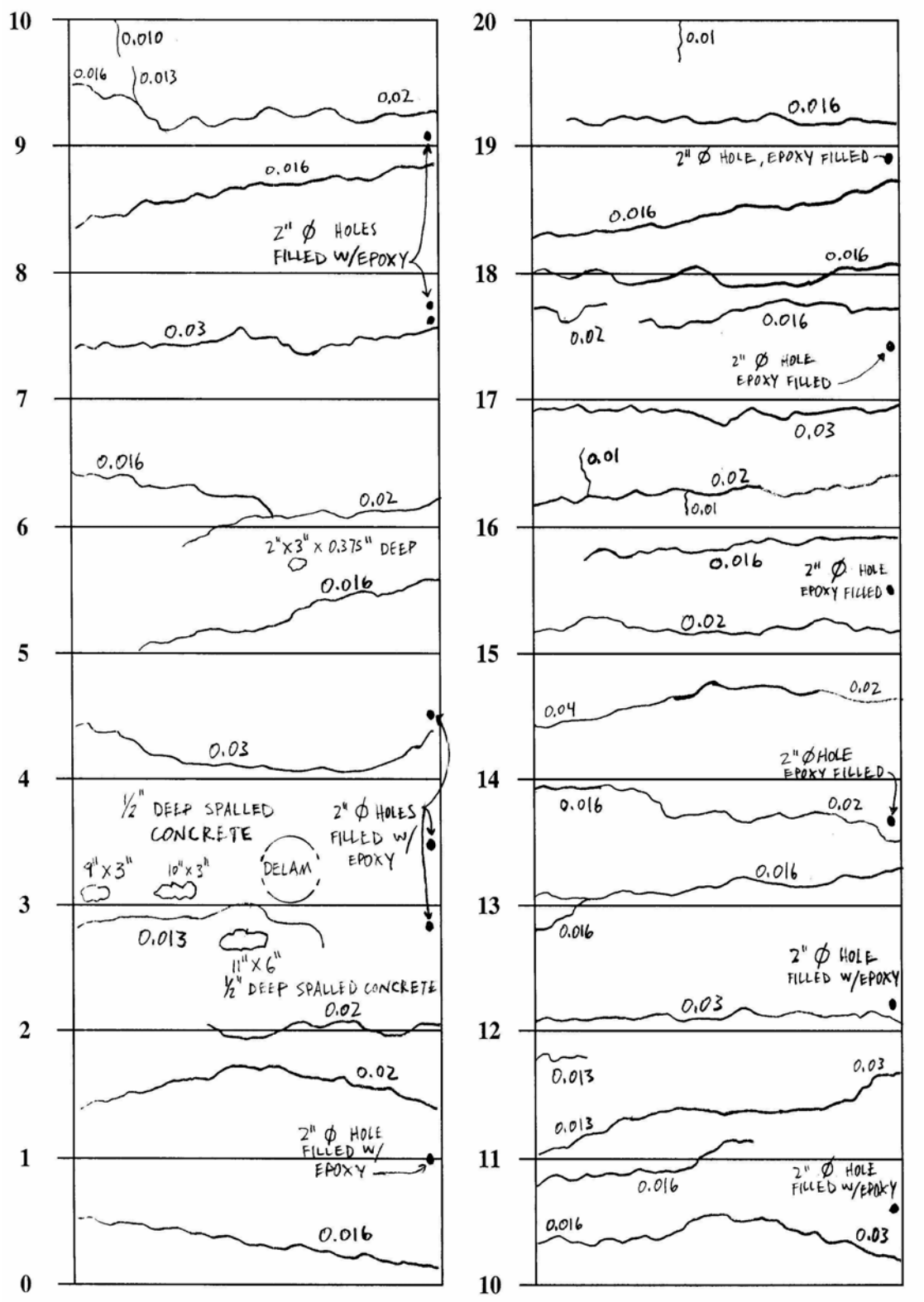

FIGURE 4.27 Distress survey of bridge C-635.

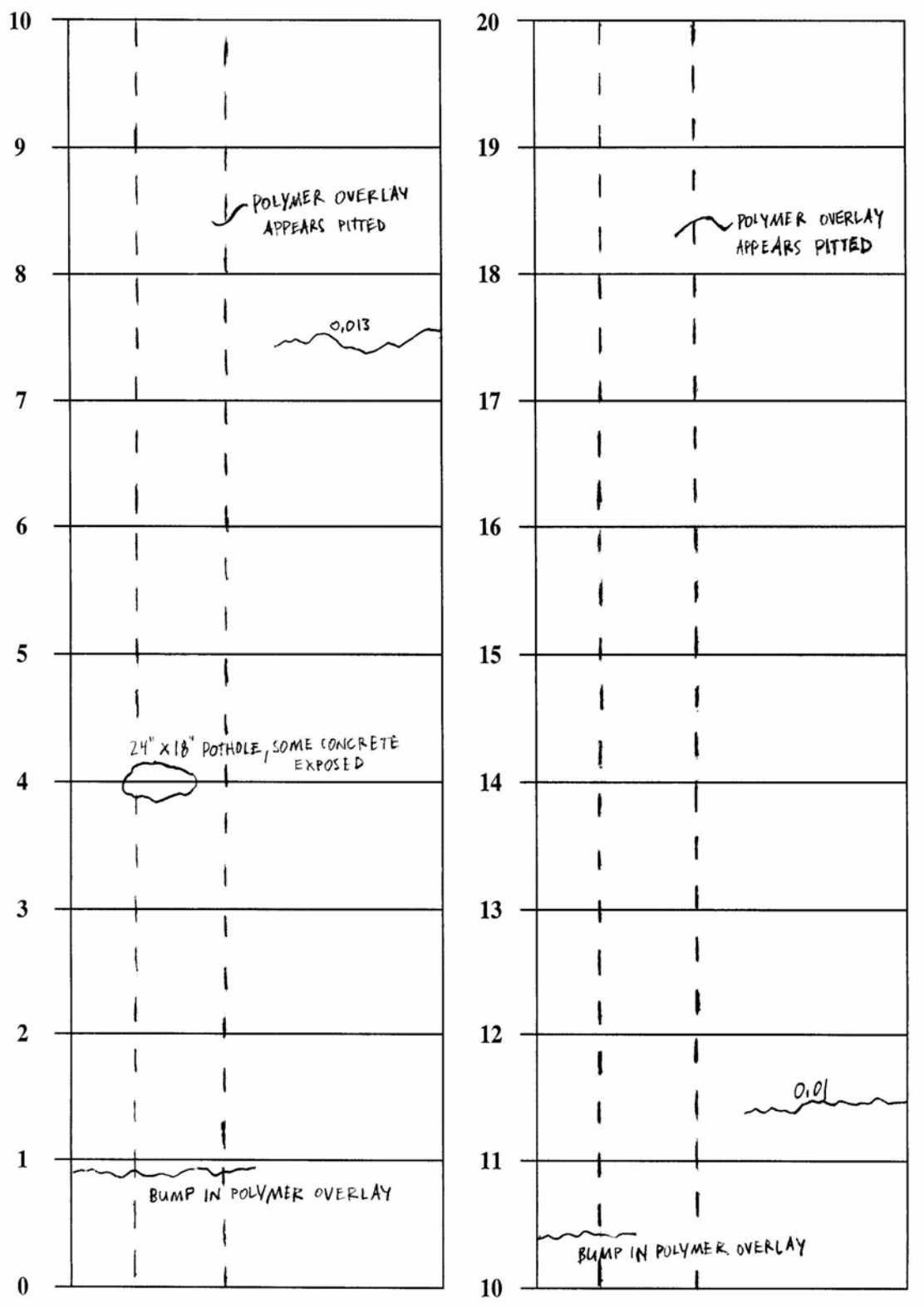

FIGURE 4.28 Distress survey of bridge C-637.

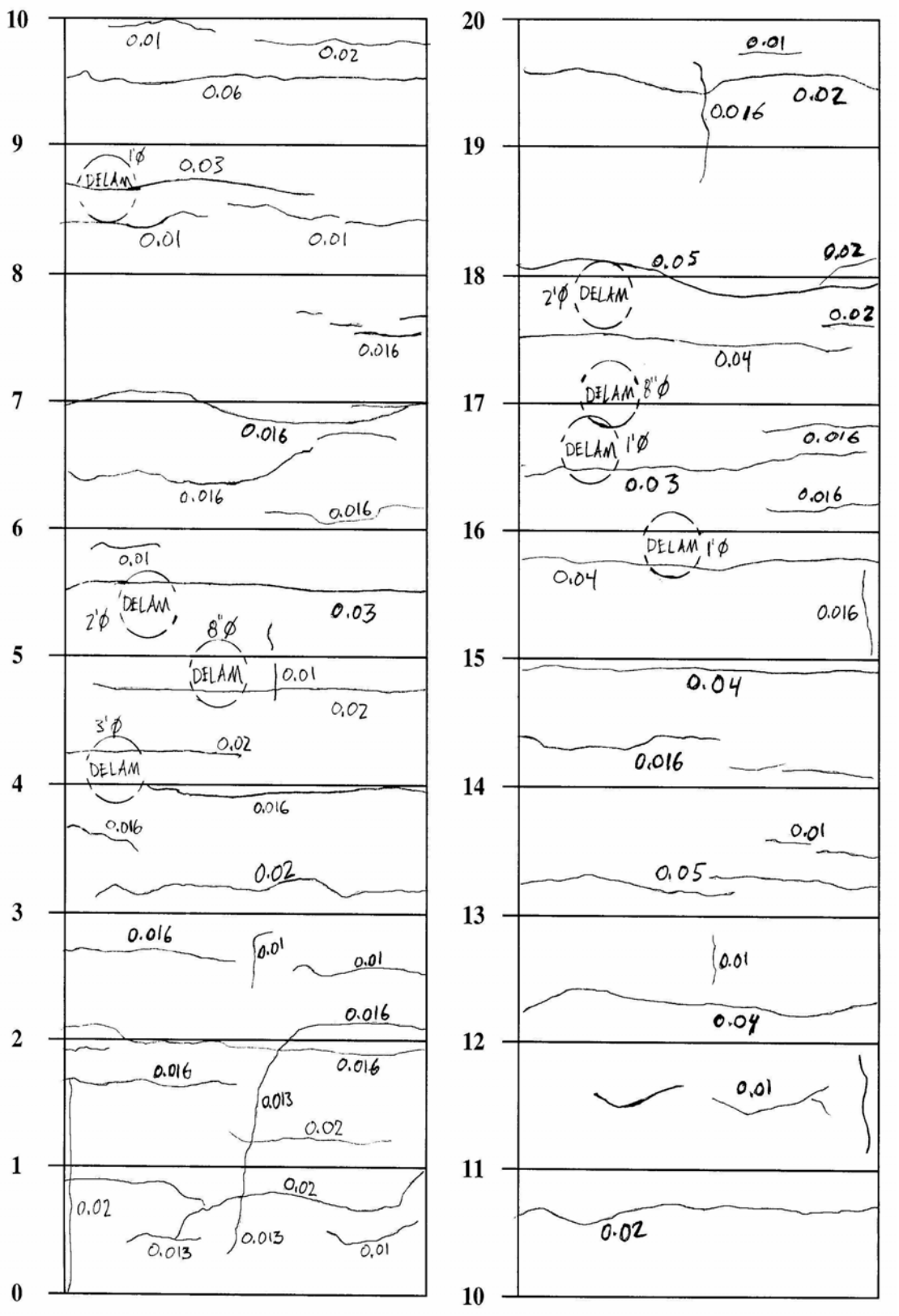

FIGURE 4.29 Distress survey of bridge C-654.

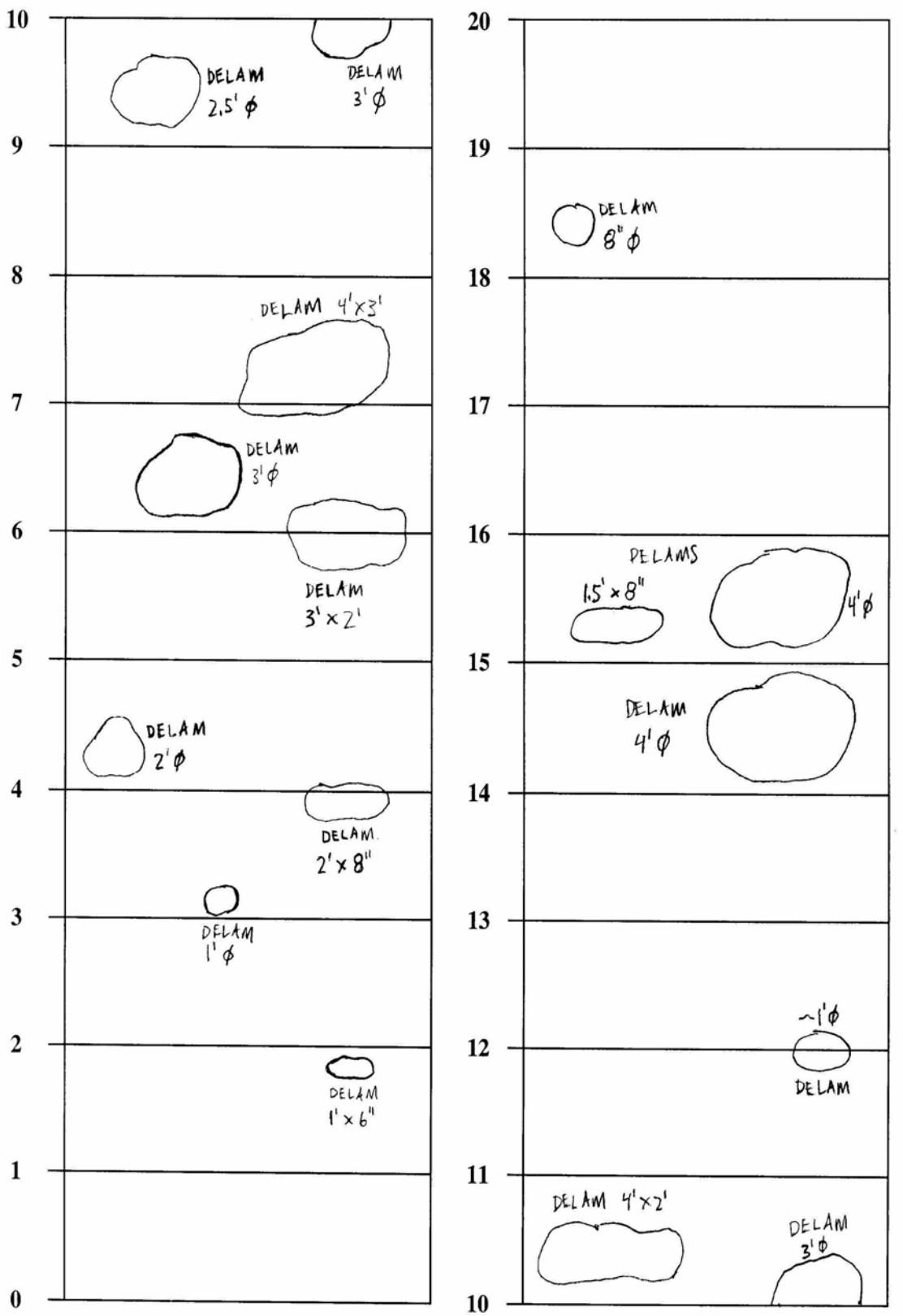

FIGURE 4.30 Distress survey of bridge C-668.

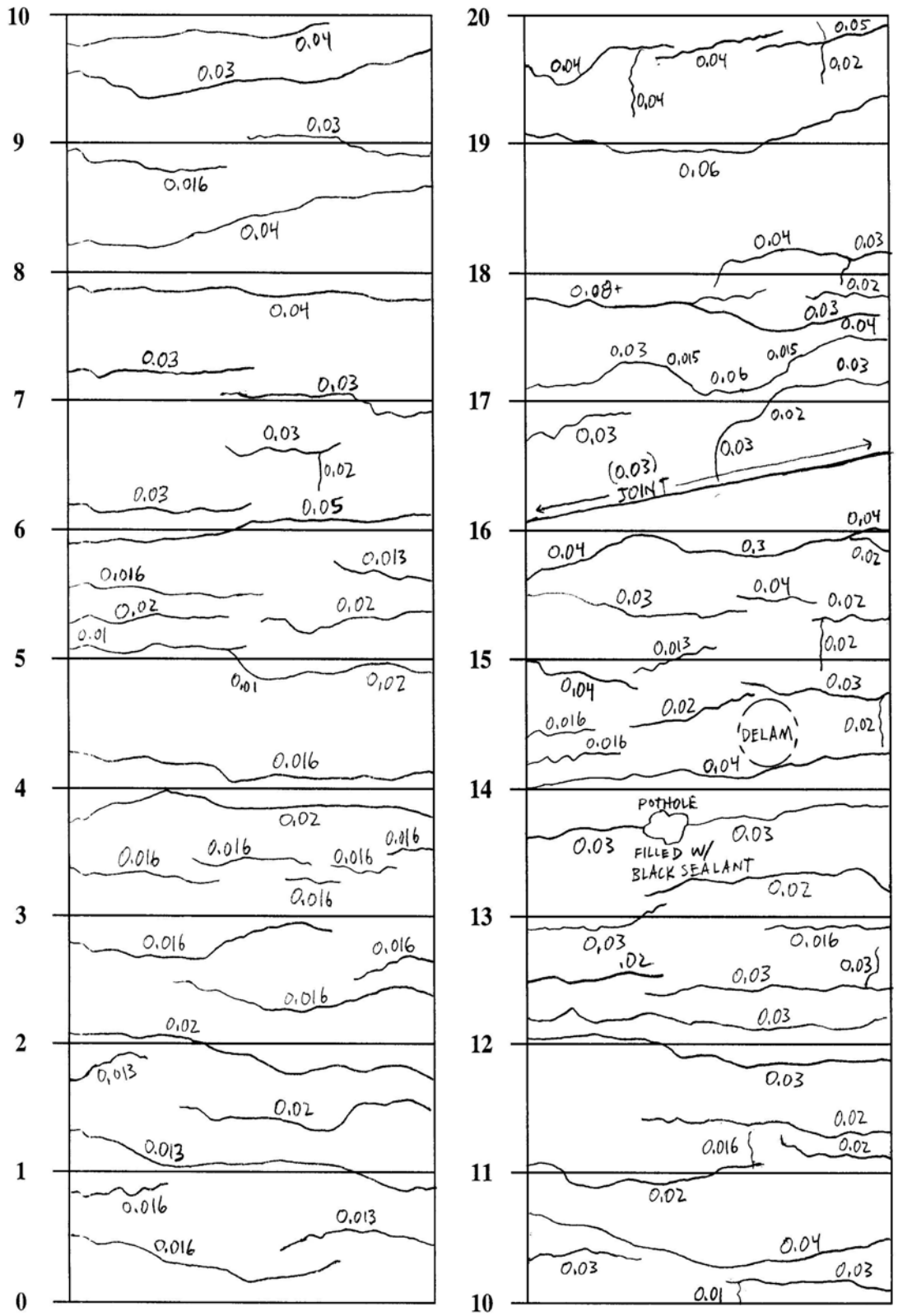

FIGURE 4.31 Distress survey of bridge C-693.

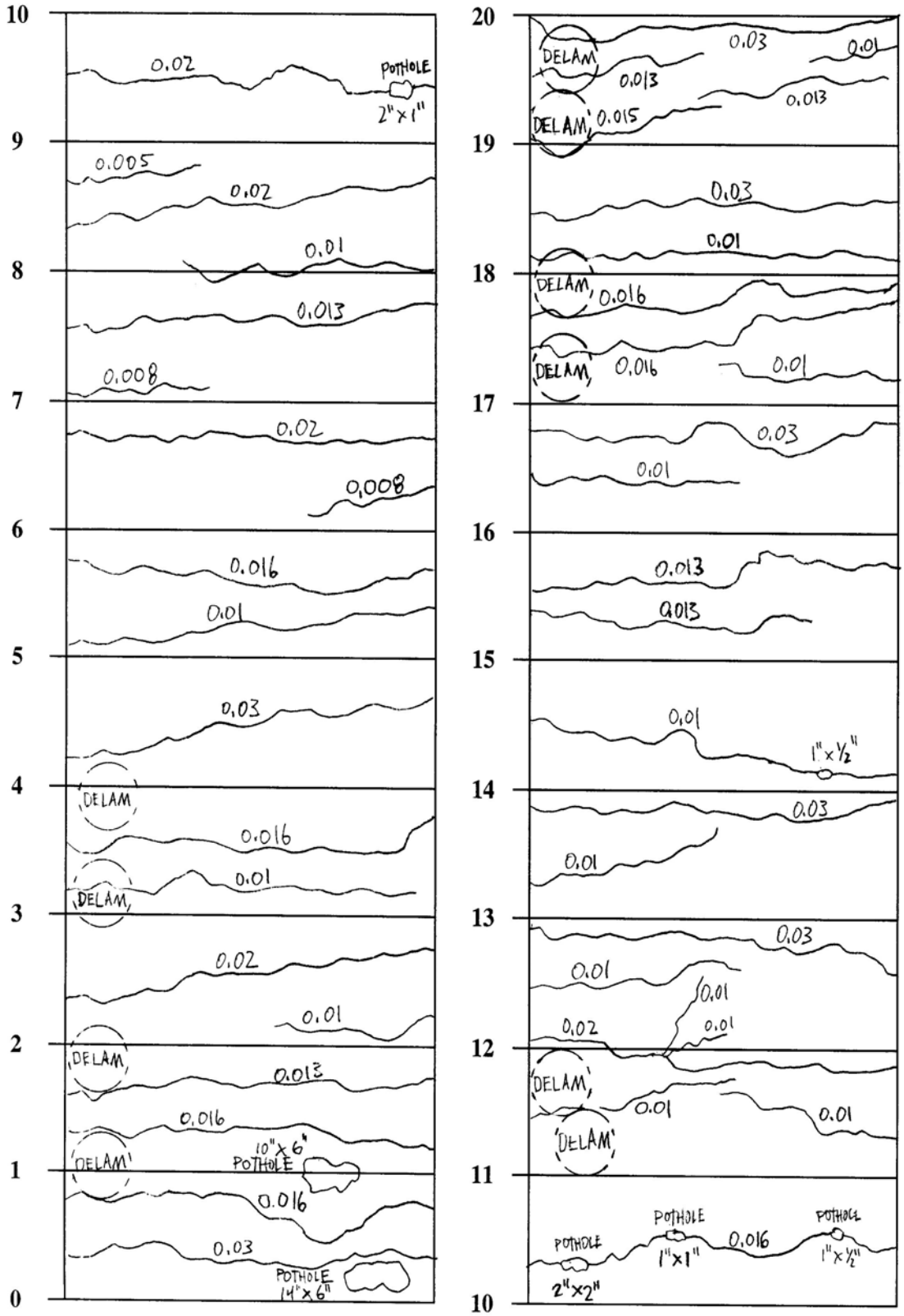

FIGURE 4.32 Distress survey of bridge C-702.

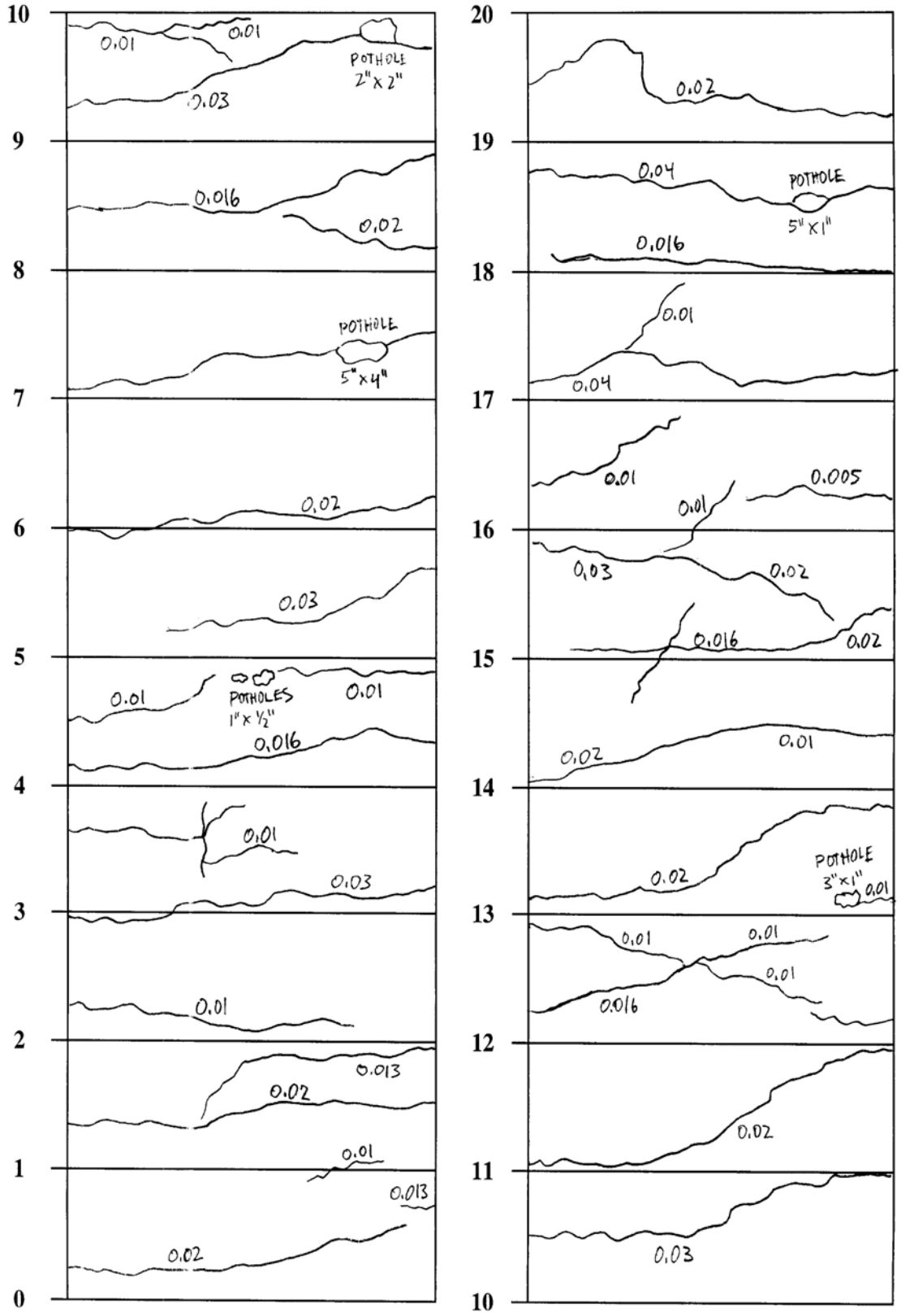

FIGURE 4.33 Distress survey of bridge C-704.

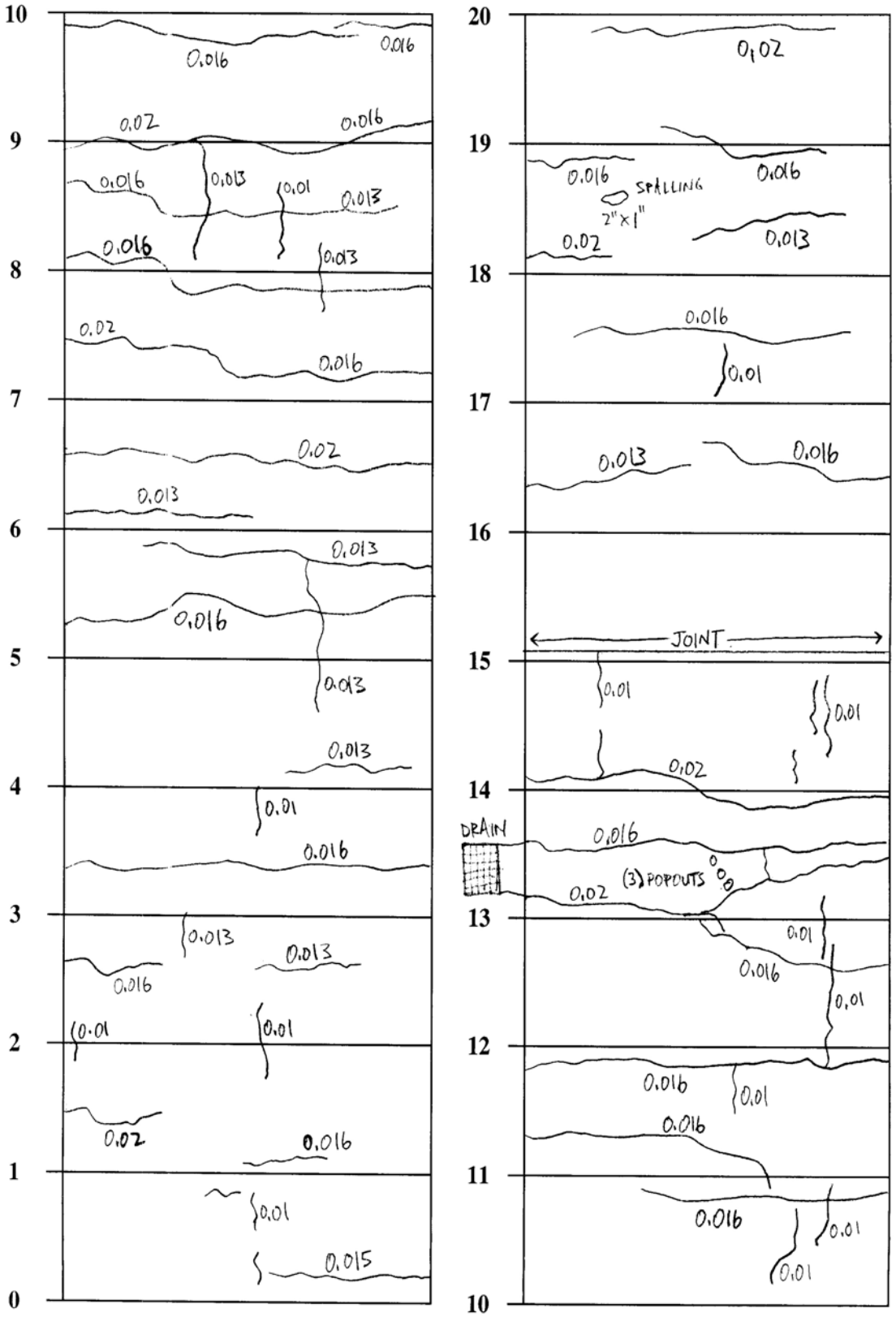

FIGURE 4.34 Distress survey of bridge C-769.

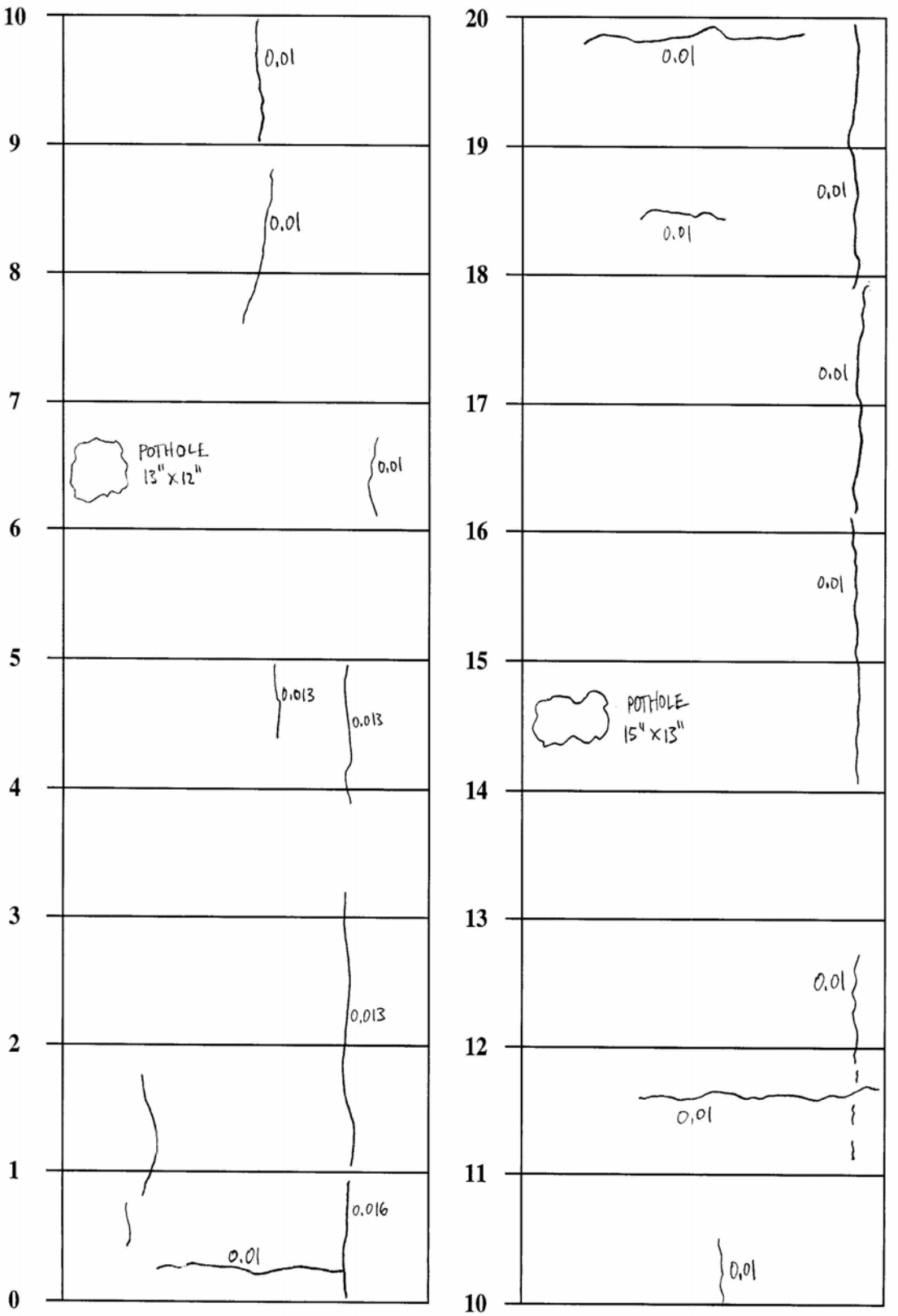

FIGURE 4.35 Distress survey of bridge F-477.

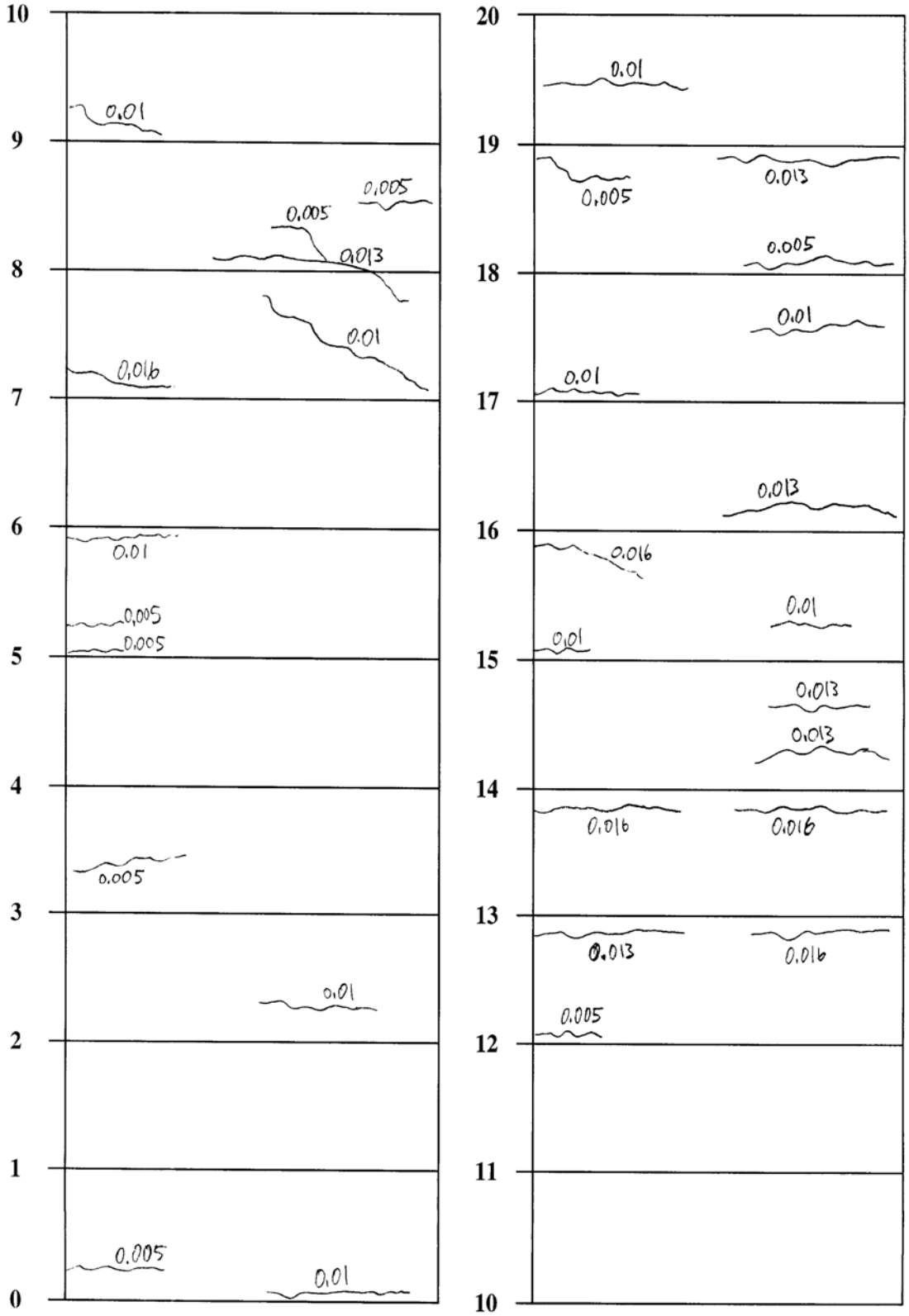

FIGURE 4.36 Distress survey of bridge F-595.

The most severe distresses manifested on the bridge decks were large transverse cracks, efflorescence in the transverse cracks, localized potholes, and multiple locations of exposed reinforcement. Figures 4.37 through 4.43 show several common distresses on the 12 bridge decks. The distresses observed on the bridge decks compare favorably with the descriptions of distresses noted in the UDOT Bridge Inspection Reports.

FIGURE 4.37 Transverse cracking and potholes on bridge C-635.

FIGURE 4.38 Exposed reinforcement in pothole on bridge C-460.

FIGURE 4.39 Transverse cracking with efflorescence on bridge C-693.

FIGURE 4.40 Localized spalling of concrete on bridge C-704.

FIGURE 4.41 Transverse cracking and potholes on bridge C-702.

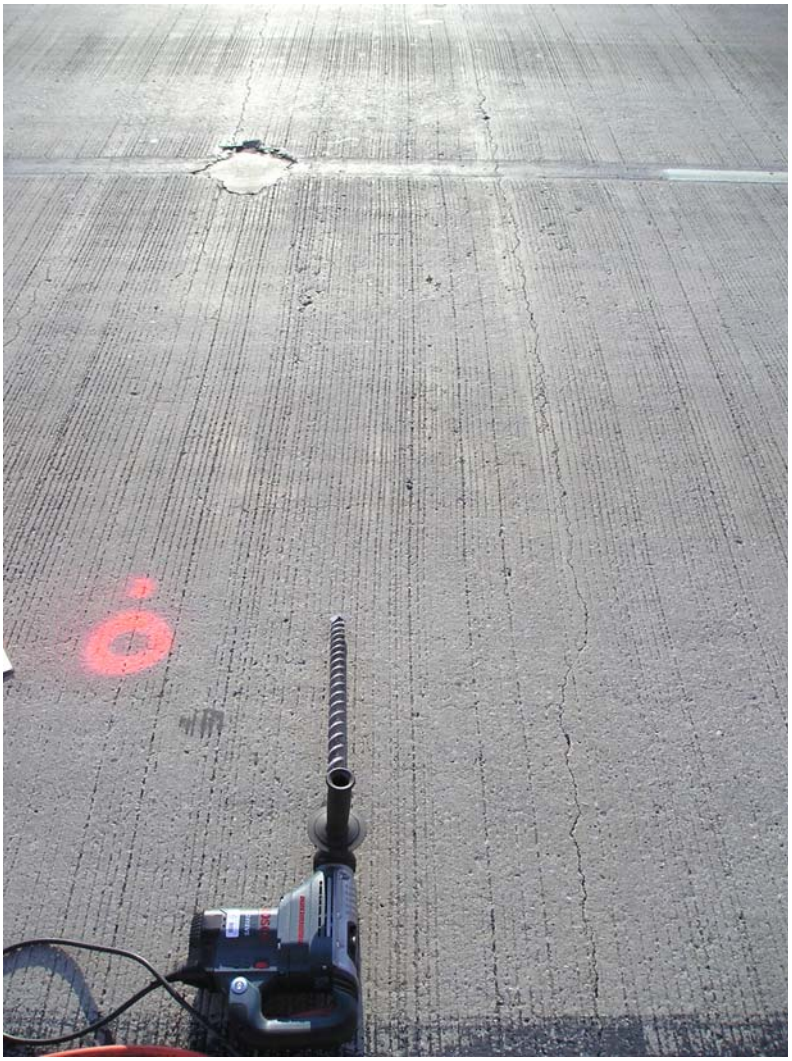

FIGURE 4.42 Transverse cracking on bridge C-460.

FIGURE 4.43 Concrete distresses exposed through overlay on bridge C-637.

4.4.1 Crack Density

Crack densities for the bridge decks, computed as the ratio of lineal cracking in feet to testing section area in square yards, are summarized in Table 4.3. Seven of the bridge decks have crack density values greater than 2 lineal feet per square yard, and two of those seven have crack densities greater than 3 lineal feet per square yard. Five bridge decks had a relatively small crack density. However, a protective overlay was placed on four of those bridge decks. Bridge F-477 had the lowest crack density among those decks not covered with a protective overlay.

An epoxy or polymer overlay was placed on bridges C-637, C-668, and F-595, and an asphalt wearing surface was placed on bridge C-493. Due to the masking effect of the protective wearing surface, the crack densities computed for these four decks are probably not accurate. Although the asphalt wearing surface of bridge C-493 was removed to facilitate visual inspection and other testing, the milling process could have altered the true surface condition of the concrete. Furthermore, the testing was performed at night when small cracks were not clearly visible. For those bridges with an epoxy or polymer overlay, only those cracks propagating through the

TABLE 4.3 Crack Density

Bridge Deck Identification	Protective Wearing Surface Overlay	Crack Density (lineal ft / yd^2)
C-460		2.58
C-493	X	0.34
C-635		2.18
C-637	X	0.09
C-654		2.76
C-668	X	-
C-693		3.69
C-702		3.09
C-704		2.40
C-769		2.23
F-477		0.58
F-595	X	0.67

protective coating were documented. The intact epoxy overlay on bridge C-668 prevented visual observation of any cracking.

4.4.2 Crack Severity

Crack severities for the tested bridge decks, calculated as the average crack width observed on the bridge decks within the testing sections, are summarized in Table 4.4. Only one bridge deck has wide cracking, nine have medium cracking, and one has narrow cracking. The crack severity could not be calculated for bridge C-668 since the epoxy overlay covered any cracks that may have been present on the deck surface.

TABLE 4.4 Crack Severity

Bridge Deck Identification	Crack Severity (in.)		Crack Width Category
	Mean	Std. Dev.	
C-460	0.018	0.006	Medium
C-493	0.040	0.014	Wide
C-635	0.018	0.006	Medium
C-637	0.010	0.003	Medium
C-654	0.021	0.012	Medium
C-668	-	-	-
C-693	0.025	0.011	Medium
C-702	0.016	0.007	Medium
C-704	0.017	0.009	Medium
C-769	0.014	0.003	Medium
F-477	0.011	0.002	Medium
F-595	0.010	0.004	Narrow

4.4.3 Pothole Density

Pothole densities for the tested bridge decks, calculated as the ratio of total pothole area in inches to the testing section area in square yards, are displayed in Table 4.5. In addition to pothole density, the number of potholes and average pothole size are documented for each deck. The average pothole area was also calculated and represents the average pothole size observed in the survey section. The values given in Table 4.5 generally corroborate the UDOT Bridge Inspection Report.

TABLE 4.5 Pothole Density

Bridge Deck Identification	Number of Potholes	Pothole Area ($in.^2$)		Pothole Density ($in.^2 / yd^2$)
		Mean	Std. Dev.	
C-460	9	217	172	17.54
C-493	5	253	507	11.38
C-635	4	32	25	1.16
C-637	1	432	-	3.89
C-654	0	-	-	-
C-668	0	-	-	-
C-693	1	192	-	1.73
C-702	7	22	35	1.36
C-704	6	7	8	0.38
C-769	1	2	-	0.01
F-477	2	140	16	2.51
F-595	0	-	-	-

4.5 DIELECTRIC MEASUREMENTS

Dielectric measurements were obtained at each station marker in the testing area on all but one bridge deck. The average dielectric values for each bridge deck are summarized in Table 4.6. Values are generally within the range typical of aggregate particles and therefore do not necessarily indicate an unusual quantity of free water in the decks. The highest value, measured on bridge C-493, was likely affected by the water applied to the deck during the milling process used to remove the asphalt overlay prior to inspection and testing. Threshold values for dielectric measurements do not exist. Dielectric values were entered in the GeoRadar software to facilitate accurate computation of deck thickness within individual GPR images.

TABLE 4.6 Dielectric Values

Bridge Deck Identification	Dielectric Value
C-460	5.9
C-493	8.2
C-635	5.7
C-637	4.2
C-654	5.9
C-668	3.6
C-693	4.5
C-702	NA
C-704	6.8
C-769	6.5
F-477	5.5
F-595	4.0

4.6 GROUND-PENETRATING RADAR IMAGING

GPR images were acquired to document a longitudinal, full-depth profile of each test section, as well as to locate and map subsurface deck features such as reinforcing steel and delaminations. In most cases, the GPR image profiles appear relatively uniform. For example, Figure 4.44 is a GPR image of bridge deck C-635, which is in good condition with no delaminations or other defects. In each GPR image, the small black squares across the tops of the images represent station markers at 5-ft increments. Station numbers increase from left to right in images 4.44 and 4.46, and right to left in image 4.45. The wave form on the right side of each plot shows the deck profile at a representative point on the deck. The largest peak identifies the top of the deck, while the second largest peak represents the bottom of the deck; the other peaks represent waves that were reflected multiple times within the concrete deck before returning to the antenna. The thin, vertical, evenly spaced reflections indicate the locations of the transverse steel reinforcement. For most decks the transverse steel was placed with 6 in. spacing.

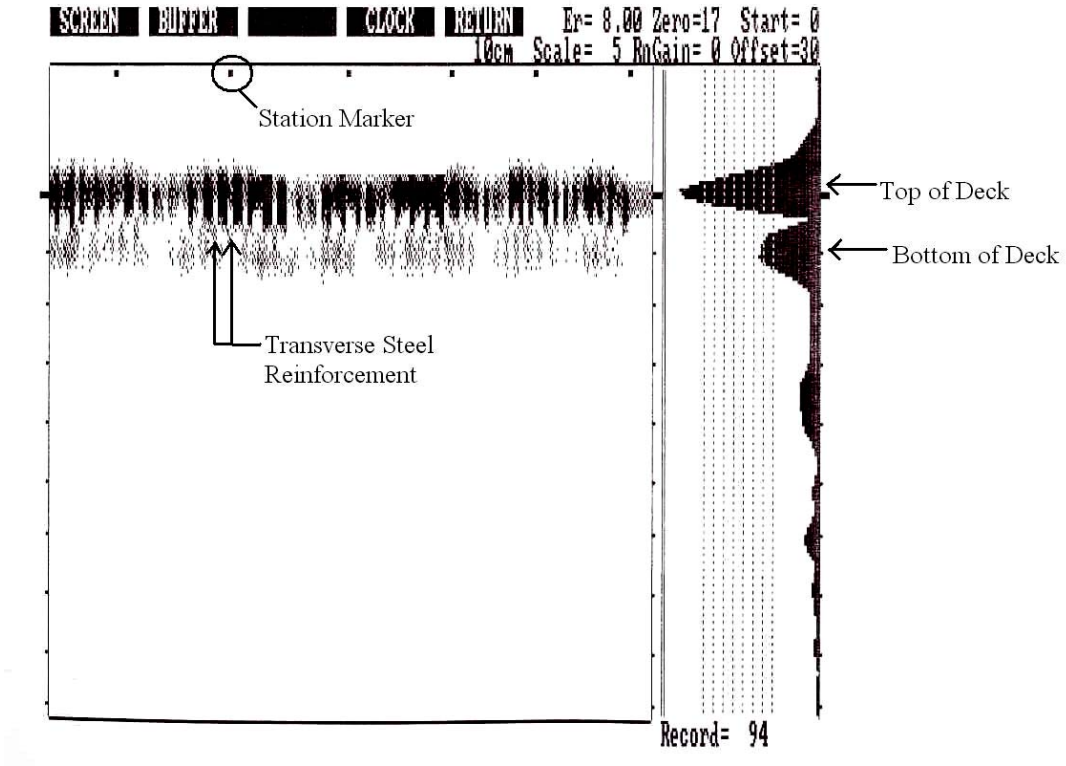

FIGURE 4.44 GPR image of deck profile on bridge C-635.

Defects in the deck were identified by aberrations in the images. The images in Figure 4.45 and Figure 4.46 illustrate examples of delaminations, which have been circled for clarification. The delamination in Figure 4.45 was identified by the vertical and horizontal gaps located between the sixth and eighth small black squares from the left. Similarly, the delamination in Figure 4.46 was identified by the abnormal vertical gap in the image near the third black square from the left. Figure 4.46 also clearly shows the spacing of the steel reinforcement in the deck. The delaminations found by GPR imaging were subsequently verified using sounding methods.

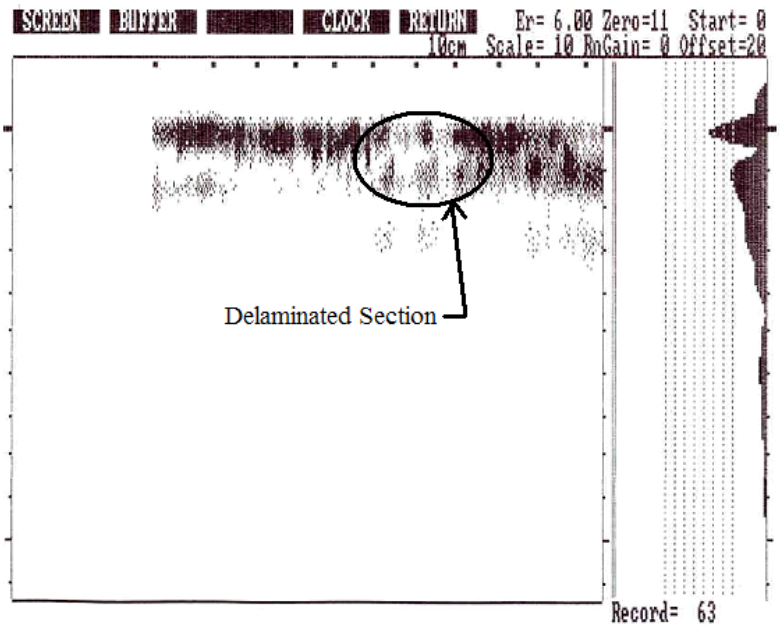

FIGURE 4.45 GPR image of a delamination on bridge C-460.

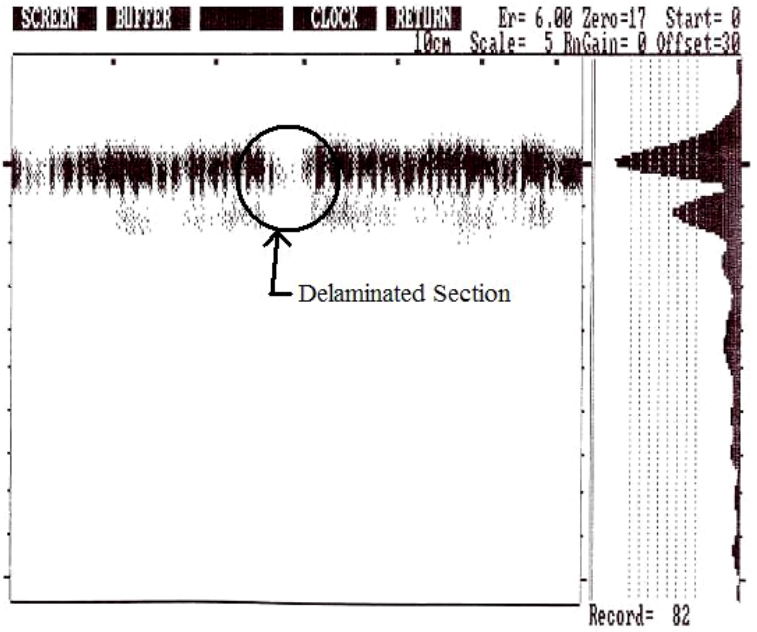

FIGURE 4.46 GPR image of a delamination on bridge C-635.

4.7 SOUNDING

Sounding methods were mainly used to locate delaminations within the testing area of each deck. Both chain dragging and hammer sounding methods proved to be highly effective in verifying delaminations detected by GPR imaging. Furthermore, because sounding was performed on the entire testing area, additional delaminations were found in areas where GPR imaging was not used. Delaminations were characterized by dull, hollow sounds, and their locations were documented on the distress maps shown in Figures 4.25 through 4.36. Because delamination sizes were difficult to assess, only the distress surveys of bridges C-654 and C-668 include estimated delamination sizes, as shown in Figures 4.29 and 4.30, respectively.

Table 4.7 summarizes the number of delaminations on each bridge deck. Five bridge decks did not have any delaminations detectable by sounding. A small number of delaminations were found on four bridge decks, and three bridge decks contained several delaminations. The delaminations identified on bridge C-668 were most likely caused by the separation of the epoxy overlay from the deck surface. Sounding often verified that delaminations were present immediately around the perimeter of potholes, suggesting that future spalling of the concrete will enlarge the potholes. Sounding proved especially

TABLE 4.7 Testing Area Delaminations

Bridge Deck Identification	Number of Delaminations
C-460	3
C-493	2
C-635	1
C-637	0
C-654	8
C-668	16
C-693	1
C-702	10
C-704	0
C-769	0
F-477	0
F-595	0

effective in locating unseen distresses on bridge decks covered with a protective wearing surface.

4.8 RESISTIVITY TESTING

The resistivity testing method used electrical resistance to evaluate the ability of the concrete covering the reinforcing steel to support corrosion current. Two measurements were taken at each station in the testing areas. An average of the two measurements was calculated to represent the resistivity value of each station. The average resistivity value for the deck was calculated using the average value at each station. The probable rates of steel reinforcement corrosion were determined by comparing the average resistivity values with the threshold values given in Table 3.2 and are shown in Table 4.8.

In consideration of the threshold values given, the results suggest that one of the bridge decks is highly likely to support corrosion, three of the bridge decks have moderate to low likelihood of supporting corrosion, and the remaining eight decks are not likely to support corrosion. However, the comparatively high standard deviations imply that some areas of the testing area would sustain higher rates of corrosion.

TABLE 4.8 Resistivity Measurements

Bridge Deck Identification	Resistivity (Ohm-in.)		Condition Assessment of Possible Corrosion
	Mean	Std. Dev.	
C-460	16694	8740	Insignificant
C-493	3626	2880	High
C-635	9452	5380	Insignificant
C-637	10272	5500	Insignificant
C-654	14580	18086	Insignificant
C-668	6427	10210	Moderate to Low
C-693	17320	7610	Insignificant
C-702	19613	12290	Insignificant
C-704	6829	3900	Moderate to Low
C-769	6931	5670	Moderate to Low
F-477	36205	2000	Insignificant
F-595	33336	7090	Insignificant

For a number of reasons, resistivity testing was not used as a primary corrosion assessment test in this research. Threshold values have not been universally established for resistivity measurements, and the high standard deviations of the results suggest that the test is not repeatable. Furthermore, because resistivity testing evaluates the quality of strictly the concrete cover, the method only provides an indirect measure of the corrosion potential of the reinforcing steel.

4.9 HALF-CELL POTENTIAL TESTING

Half-cell potential measurements were taken to determine the severity of steel corrosion in the concrete bridge decks. Two measurements were taken at each station in the testing areas. The average of these two measurements was compared to the threshold values provided in ASTM C 876. The average half-cell potential measurements for each deck were calculated from the average value of each station and are summarized in Table 4.9. Based on the threshold value of -0.35 V, the probability is greater than 90 percent that the steel reinforcement in nine bridge decks is actively corroding. Corrosion in two bridge decks is uncertain, and only one bridge deck can be classified with 90 percent reliability as inactive.

TABLE 4.9 Half-Cell Potential Measurements

Bridge Deck Identification	Epoxy-Coated Steel	Electrical Continuity	Half-Cell Potential (V)		Condition Assessment
			Mean	Std. Dev.	
C-460	X	X	-0.41	0.04	Active
C-493		X	-0.44	0.12	Active
C-635	X	X	-0.45	0.08	Active
C-637		X	-0.35	0.05	Active
C-654		X	-0.37	0.07	Active
C-668	X	X	-0.26	0.06	Uncertain
C-693	X		-0.42	0.07	Active
C-702	X	X	-0.41	0.05	Active
C-704	X	X	-0.59	0.04	Active
C-769	X		-0.22	0.05	Uncertain
F-477	X		-0.18	0.00	Inactive
F-595	X		-0.51	0.02	Active

Due to the high percentage of tested bridge decks categorized as having active corrosion, the benefit of epoxy coatings is placed in question. Because epoxy coatings should ideally prevent electrical continuity between individual reinforcing bars and the surrounding concrete, corrosion should not readily occur. However, the data collected in this research suggest that the epoxy coating on the reinforcement did not provide the expected protection. Five of the nine bridge decks with epoxy-coated steel had electrically continuous reinforcement throughout the full length of the 100-ft test section, and six of the nine were categorized as having active corrosion. The corrosion of only one bridge deck with epoxy-coated reinforcement was classified as inactive. The three bridge decks without epoxy-coated reinforcement had an electrically continuous reinforcement mat, as expected, and were all categorized as having active corrosion.

4.10 CHLORIDE CONCENTRATIONS

Chloride concentration results report the amount of free chlorides and a portion of the bound chlorides in the concrete at the depth just above the top of the steel reinforcement. For this test, two locations at opposite ends of the testing area were drilled to collect pulverized samples. Samples were collected at incremental depths until the depth of the steel was reached. The incremental samples were used to generate chloride concentration profiles for each deck and to compute the concentration gradient, or the rate at which the chloride concentration changes with depth. The steel is considered to be in a corrosive environment if the chloride concentration exceeds 2 pounds of chlorides per cubic yard of concrete. The chloride concentrations reported in Table 4.10 were obtained by testing the concrete sample collected from just above the steel reinforcement. The average chloride concentration reported for each deck was calculated using the samples closest to the steel at the two locations within the testing area. Also provided in Table 4.10 is the average concentration gradient for each deck, the average depth to the steel reinforcement, and the number of locations drilled on each deck. Where the standard deviation is not shown, only one test hole was drilled on the deck instead of two, or only one calculation was possible.

The results imply that 11 bridge decks have chloride concentration levels that would positively support corrosion. Only bridge F-477 does not exceed the minimum

TABLE 4.10 Average Chloride Concentration and Concentration Gradient

Bridge Deck Identification	Steel Depth (in.)		Chloride Concentration ($lbs\ Cl^-$) / (yd^3 Concrete)		Concentration Gradient ($lbs\ Cl^-$ / yd^3Concrete) / (in. Depth)	
	Mean	St. Dev.	Mean	St. Dev.	Mean	St. Dev.
C-460	1.1	0.2	16.8	0.7	15.7	-
C-493	2.8	-	12.2	-	-	-
C-635	2.6	-	9.9	-	8.9	-
C-637	2.7	-	10.0	-	5.1	-
C-654	2.0	-	8.3	-	4.9	-
C-668	2.0	0.5	12.1	6.8	6.8	0.8
C-693	2.5	0.1	5.1	6.8	20.0	2.5
C-702	2.4	0.3	13.9	3.7	7.4	2.4
C-704	2.9	0.1	14.5	0.1	7.1	0.3
C-769	2.7	0.5	6.1	4.1	14.5	6.1
F-477	2.2	0.0	0.4	0.3	15.4	0.8
F-595	2.1	0.0	5.7	3.2	5.6	1.1

amount of chlorides necessary to initiate corrosion; however, the concentration gradient computed for that bridge suggests that high chloride concentrations are present within the concrete cover that will inevitably diffuse down to the depth of the steel reinforcement. That is, even if immediate action were taken to cover the deck with a protective overlay so as to prevent further chloride penetration, sufficient chlorides currently exist in the deck to cause future damage. Further research would have to be conducted to estimate the chloride diffusion rate for this deck and then predict the time at which corrosion would begin. Infiltration of chlorides through the concrete clear cover and their accumulation at the level of the steel is clearly one of the leading causes of cracking, potholes, and delaminations characteristic of the bridge decks investigated in this study.

Eleven of the bridge decks meet the 2-in. minimum concrete clear cover required by UDOT at the time the decks were constructed; the minimum cover required by UDOT has been recently increased to 2.5 in., however. The deficient cover in bridge C-460 has led to a significant concentration of chlorides at the depth of the steel reinforcement, and the infiltration of chlorides has subsequently initiated corrosion of the steel, as depicted from half-cell potential measurements, and caused numerous delaminations, increased amounts of cracking, and potholes with exposed reinforcement. Therefore, inadequate

concrete cover proved to be one of the leading causes of deck deterioration on bridge C-460.

4.11 SUMMARY

The method currently utilized by UDOT to rate the condition of Utah bridge decks is based on a subjective, numerical condition score derived entirely from visual inspection of the wearing surface and the concrete deck structure. Several testing techniques were employed in this research to assess not only the current condition of the bridge decks, but also the probability of future damage. Evaluation techniques included visual inspection, sounding, dielectric measurements, GPR imaging, half-cell potential testing, resistivity testing, and chloride concentration analysis. Results from these tests provided a more thorough diagnosis of the condition of the bridge decks and the potential to support corrosion of the reinforcing steel. A complete diagnosis of each bridge deck is given in Table 4.11.

Table 4.11 Summary of Bridge Deck Condition Analysis

Bridge Number	Age (years)	NBI Deck Rating (0 - 9)	Percent Tested (%)	Wearing Surface Overlay	Crack Density (ft / yd^2)	Crack Severity	Number of Potholes	Pothole Density (in.^{2} / yd^2)	Number of Delami-nations	Resistivity Corrosion Assessment	Epoxy-Coated Steel	Electrically Continuous Steel	Half-Cell Corrosion Assessment	Chloride Concentration (lbs Cl$^-$) / (yd^3 Concrete)	Chloride Concentration Gradient (lbs Cl$^-$ / yd^3 Concrete) / (in.)
C-460	17	7	2.8		2.58	Medium	9	17.54	3	Insignificant	X	X	Active	16.8	15.7
C-493	30	4	1.5	X	0.34	Wide	5	11.38	2	High		X	Active	12.2	-
C-635	23	7	6.6		2.18	Medium	4	1.16	1	Insignificant	X	X	Active	9.9	8.9
C-637	19	6	3.1	X	0.09	Medium	1	3.89	0	Insignificant		X	Active	10.0	5.4
C-654	26	7	31.9		2.76	Medium	0	0	8	Insignificant		X	Active	8.3	4.9
C-668	19	6	6.1	X	-	-	0	-	16	Moderate to Low	X	X	Uncertain	12.1	6.1
C-693	22	7	2.9		3.69	Medium	1	1.73	1	Insignificant	X		Active	5.1	19.7
C-702	20	6	11.2		3.09	Medium	7	1.36	10	Insignificant	X	X	Active	13.9	6.9
C-704	20	6	1.4		2.40	Medium	6	0.38	0	Moderate to Low	X	X	Active	14.5	7.1
C-769	14	7	4.7		2.23	Medium	1	0.01	0	Moderate to Low	X		Uncertain	6.1	14.5
F-477	17	7	3.9		0.58	Medium	2	2.51	0	Insignificant	X		Inactive	0.4	15.5
F-595	9	7	5.9	X	0.67	Narrow	0	0	0	Insignificant	X		Active	5.7	5.6

Referring to the deck condition rating, seven of the bridge decks are in good condition, four are in satisfactory condition, and one is in poor condition. The ratings adequately represent current deck condition according to visual inspections conducted by UDOT, except for bridges C-460 and C-704. The notes recorded at the time of the inspections give further insights pertaining to the condition ratings of those decks.

BYU researchers utilized visual inspection, sounding, and GPR imaging to quantify the current evidence of deterioration manifest on the bridge decks. The potential for corrosion was assessed using resistivity testing, half-cell potential testing, and chloride concentration measurements. These additional non-destructive tests suggest that all of the tested deck areas except bridge F-477 are experiencing active corrosion. To the extent that the testing areas are representative of the entire deck areas, this conclusion may be applied to the decks generally. That is, if the tested and untested areas of each bridge deck are in similar condition, the collected data may be considered a reliable indicator of the overall deck condition.

The results of the condition assessment testing indicate that all 12 of the bridge decks are in a condition beyond which preventive maintenance can be effectively applied, and 11 of the 12 bridge decks are in a condition beyond which rehabilitation can be effectively applied; for these 11 decks, the only alternative is replacement. Even though replacement is recommended, not all of the bridge decks have reached the end of their service life. Corrective maintenance techniques may prolong the service life of these bridges until unserviceable conditions are reached.

The only deck that does not currently appear to be experiencing active steel corrosion is bridge F-477. Because excessive chlorides are already present in the concrete cover, however, the time at which critical chloride concentrations will be reached depends only upon the rate of chloride diffusion through the concrete. In this case, two rehabilitation techniques are suggested. One alternative is to mill and replace the top deck surface to the depth of the upper mat of reinforcing steel in order to remove chlorides and minimize further chloride-induced corrosion; a low-permeability overlay should be specified for this application. Another alternative is to use an electrochemical chloride extraction technique. The latter procedure, however, may require bridge closure for several weeks compared to a number of days for milling and overlay construction.

Based on data collected and analyzed in this research, UDOT engineers should plan to program all of the tested bridge decks, except bridge F-477, for replacement when the ride quality or structural integrity of the bridge decks can no longer be maintained at a reasonable cost. Bridge F-477 may be effectively rehabilitated using the mill-and-overlay approach if performed before chloride concentrations exceed critical values at the level of the reinforcing steel.

CHAPTER 5
CONCLUSION

5.1 SUMMARY

UDOT is responsible for 1,700 bridges throughout the state, of which 46 percent are older than 30 years. Because of the comparatively high number of bridges approaching the end of their service lives, UDOT engineers are interested in developing a protocol for objectively and reliably assessing the condition of concrete bridge decks in order to optimize MR&R actions.

While threshold values for various non-destructive condition assessment methods were proposed in earlier UDOT research performed at BYU, this work focused on implementing the recommended test criteria. Because the previous research identified corrosion of reinforcing steel as the primary cause of concrete bridge deck damage, this research especially investigated non-destructive testing techniques that can be used to estimate the extent of corrosion activity occurring within the bridge deck before damage is visually apparent on the deck surface in the form of cracking, delaminations, or potholes. The condition assessment methods used by BYU researchers include visual inspection, hammer sounding and chaining, dielectric measurements, GPR imaging, resistivity testing, half-cell potential testing, and chloride concentration measurements.

Research performed in this study considered 12 concrete bridge decks of various age and condition, all generally located in northern Utah. UDOT inspection reports from bridges tested in this research were used in conjunction with the results of non-destructive testing to establish the condition and corrosion potential of the bridge decks. The bridge deck condition analyses produced from the results of non-destructive testing were compared to the visual inspection ratings assigned to each deck by UDOT.

Depending on the extent and severity of deterioration manifest on each deck, a recommendation to rehabilitate or replace each tested bridge deck was provided.

5.2 FINDINGS

Inspection notes archived by UDOT bridge inspectors provided numerous details of visual distresses manifest on the bridge decks. Distresses observed by UDOT bridge inspectors included full-depth transverse cracking with light to heavy efflorescence in 11 of the bridge decks, longitudinal cracking in two of the bridge decks, potholes in four of the bridge decks, and delaminations in two of the bridge decks. The condition of the decks reported by UDOT bridge inspectors correspond well with the deck condition rating assigned to each bridge, with two exceptions in which the bridge deck ratings were not comparable to the component ratings given to the wearing surface and deck structure.

The non-destructive testing provided supplemental data for assessing the condition of the bridge decks. Visual inspections facilitated creation of distress maps, which marked the extent and severity of cracking, potholes, and delaminations. Data from the visual inspections were used to calculate crack density, crack severity, and pothole density. All of the bridge decks free of a protective overlay contained numerous transverse cracks of various widths and lengths; limited cracking was visible on those bridge decks with overlays due to the masking effect of the wearing surfaces. Only small amounts of longitudinal cracking were observed.

Sounding techniques and GPR imaging detected the presence of delaminations in seven of the bridge decks, although sounding techniques were generally more effective in finding delaminations than GPR imaging. The number of delaminations detected by sounding was much greater than the number of delaminations reported by UDOT bridge inspectors.

Through resistivity testing, the probability of corrosion of the reinforcing steel was determined to be insignificant in eight of the bridge decks, moderate to low in three of the bridge decks, and high in one bridge deck. However, relatively high standard deviations associated with the resistivity measurements suggest that the reinforcing steel in many areas of the decks is probably corroding at much higher rates. Resistivity testing

was not used as a primary corrosion assessment test due to high standard deviations, non-standardized threshold values, and its inability to test the corrosion of the steel directly.

Half-cell potential measurements indicate that nine bridge decks are experiencing active steel corrosion, while only one is not experiencing corrosion; the corrosion potentials of the remaining two decks are uncertain. Of the nine actively corroding decks, only three do not have epoxy-coated steel reinforcement. Therefore, the epoxy-coated steel mats in six of the bridge decks have deteriorated to a point where corrosion currents can flow between the steel and the surrounding concrete. Of these six, five were found to have a continuous steel matrix throughout the testing area, suggesting that corrosion current can also flow between individual reinforcement bars. Both of the bridge decks with uncertain corrosion also have epoxy-coated reinforcement. The corrosion of only one bridge deck with epoxy-coated reinforcement was classified as inactive. These data suggest that the epoxy coating applied to the steel reinforcement on the tested decks is not providing significantly greater protection from corrosion than that afforded by plain black bar.

Chloride concentration measurements at a depth just above the steel reinforcement provide conclusive evidence that the application of deicing salts during winter maintenance operations is a primary cause of deck deterioration in Utah. Eleven of the 12 tested bridge decks have chloride concentrations well above the accepted threshold value of 2 pounds of chloride per cubic yard of concrete needed to initiate corrosion, and the high chloride concentration gradient for the remaining deck suggests that sufficient chlorides currently exist in the deck to cause future damage even if the deck were immediately surfaced with a protective overlay.

Inadequate reinforcing concrete cover is one of the leading causes of distresses and increased deterioration of the concrete decks. The deficient cover in one bridge deck, when compared to the other bridges, lead to increased numbers of potholes and delaminations, greater crack density and severity, lower resistivity in some areas, more negative half-cell potential readings, and higher chloride concentrations at the depth of the steel reinforcement.

The non-destructive testing methods performed on the 12 bridge decks demonstrated an ability to accurately identify and assess the internal conditions of the

concrete and reinforcing steel that are sustaining corrosion. Although resistivity testing assessed the ability of the concrete to support corrosion, it was not as likely as half-cell potential and chloride concentration testing to detect a deteriorating bridge deck.

5.3 RECOMMENDATIONS

The results produced from this research lead to several recommendations. Deck conditions of all 12 bridges tested in this study have deteriorated beyond the point at which preventive maintenance action would be effective, and only one of the bridge decks is eligible for rehabilitation. Rehabilitation of the remaining eleven bridge decks would not likely produce a substantial increase in service life due to the high chloride concentrations present in the vicinity of the reinforcing steel. Therefore, the bridge decks should be maintained through corrective maintenance treatments as needed until replacement becomes necessary. As mentioned earlier, these recommendations are valid only to the extent that the testing areas are representative of the entire deck surfaces. Before MR&R action is taken, further testing of specific decks of interest should be conducted to confirm that these conclusions are reliable and applicable.

Future concrete bridge deck condition assessments conducted by UDOT should include visual inspection, sounding, half-cell potential measurements, and chloride concentration testing for determining whether a deteriorating deck should be rehabilitated or replaced, or whether application of a preventive maintenance treatment to a relatively new deck is appropriate; dielectric measurements, GPR imaging, and resistivity testing are not as valuable for determining bridge deck condition. While threshold values for half-cell potential and chloride concentration testing have been established, UDOT should consider developing meaningful threshold values for crack density, crack severity, and pothole density.

Quantitative analyses, such as a comparison of crack density to half-cell potential or age to chloride concentration, should also be conducted to evaluate relationships among the results of different test methods at a given point in time, as well as the relationships among various testing methods and bridge age. The effects on deck deterioration rates of specific aspects of construction, such as concrete cover, or environmental conditions, such as temperature, humidity, and salinity, should also be

determined. Ultimately, relating causative factors to performance characteristics will enable development of meaningful numerical models for predicting bridge service life and determining the optimum timing for MR&R actions.

In order to implement these recommendations, UDOT will need to develop new bridge inspection and testing protocols. These protocols will require the purchase of new equipment, training of bridge inspectors, alteration of the existing BMS database so that supplementary test results can be included, and assurance of funding so that MR&R action can be implemented when signaled by the new performance indicators. Additional testing and development of deterioration and predictive models for life-cycle cost analysis of bridge decks would greatly benefit UDOT engineers responsible for programming MR&R actions for Utah bridges.

REFERENCES

1. National Bridge Inventory Study Foundation, Utah State Summary. http://www.nationalbridgeinventory.com/nbi_report_200441.htm. Accessed September 15, 2004.

2. Hema, J., W. S. Guthrie, and F. Fonseca. *Concrete Bridge Deck Condition Assessment and Improvement Strategies.* Report UT-04-16. Department of Civil and Environmental Engineering, Brigham Young University, Provo, UT, 2005.

3. Hudson, S. W., R. F. Carmichael III, L. O. Moser, W. R. Hudson, and W. J. Wilkes. Bridge Management Systems. In *Transportation Research Record 300*, TRB, National Research Council, Washington, DC, 1987, pp. 5.

4. Adams, T. M., J. A. Pincheira, and Y.-H. Huang. *Assessment and Rehabilitation Strategies/Guidelines to Maximize the Service Life of Concrete Structures*. Wisconsin Highway Research Program #0092-00-17. Wisconsin Department of Transportation, Madison, WI, 2002.

5. Hawk, H. *Bridge Life-Cycle Cost Analysis*. NCHRP Report 483. NCHRP, TRB, National Research Council, Washington, DC, 2003.

6. Guthrie, W. S. *Data Considerations for Pavement Management Systems*. Division of Materials Engineering, Texas A&M University System, College Station, TX, 2001.

7. *Recording and Coding Guide for the Structure Inventory and Appraisal of the Nation's Bridges.* Report No. FHWA-PD-96-001. United States Department of Transportation, Federal Highway Administration, Washington DC, December 1995.

8. http://www.dictionary.com. Accessed April 4, 2005.

9. Mindess, S., J. F. Young, and D. Darwin. *Concrete*, Second Edition. Pearson Education, Inc., Upper Saddle River, NJ, 2003.

10. Hudson, W. R., R. Haas, and W. Uddin. *Infrastructure Management*. McGraw-Hill, New York, NY, 1997.

11. Manning, D. G. *Detecting Defects and Deterioration in Highway Structures*. National Cooperative Highway Research Program Synthesis of Highway Practice 118. NCHRP, TRB, National Research Council, Washington, DC, 1985.

12. Shin, H., and D. A. Grivas. *How Accurate is Ground-Penetrating Radar (GPR) for Bridge Deck Condition Assessment?* Department of Civil and Environmental Engineering, Rensselaer Polytechnic Institute, Troy, NY, 2003.

13. Henderson, M. E., G. N. Dion, and R. D. Costley. Acoustic Inspection of Concrete Bridge Decks. In *SPIE Conference on Nondestructive Evaluation of Bridges and Highways III*, Newport Beach, CA, March 1999, pp. 219-227.

14. *Concrete Bridge Deck Performance*. National Cooperative Highway Research Program Synthesis of Highway Practice 333. NCHRP, TRB, National Research Council, Washington, DC, March 2005.

15. Stratfull, R. F. Corrosion Autopsy of a Structurally Unsound Bridge Deck. In *Highway Research Record 433*, HRB, National Research Council, Washington, DC, 1973, pp. 1-11.

16. Gucunski, N., S. Antoljak, and A. Maher. Seismic Methods in Post Construction Condition Monitoring of Bridge Decks. In *Use of Geophysical Methods in Construction*, Special Publication No. 108, 2000, pp. 35-51.

17. Moore, W. Detection of Bridge Deck Deterioration. In *Highway Research Record 451*, HRB, National Research Council, Washington, DC, 1975, pp. 53-61.

18. Guthrie, W. S., P. Ellis, and T. Scullion. Repeatability and Reliability of the Tube Suction Test. In *Transportation Research Record 1772,* TRB, National Research Council, Washington, DC, 2001, pp. 151-157.

19. Conyers, L. What is G.P.R.? Anthropology Department, University of Denver, Denver, CO. http://www.du.edu/~lconyer/. Accessed August 25, 2003.

20. Maser, K. R. *Use of Nondestructive Evaluation for Large Scale Bridge Deck Evaluation*. In proceedings of the Second International Symposium on Maintenance and Rehabilitation of Pavements and Technological Control, Auburn, AL, July 2001.

21. Sharma, P. V. *Environmental and Engineering Geophysics*. Cambridge Printing Press, Cambridge, United Kingdom, 1997.

22. Stratfull, R. F. Half-Cell Potentials and the Corrosion of Steel in Concrete. In *Highway Research Record 433*, HRB, National Research Council, Washington, DC, 1973, pp. 12-21.

23. Finch, R., R. Fischer, M. Grimes, R. Stits, and W. A. Watkins. *Acceptable Methods, Techniques, and Practices—Aircraft Inspection and Repair, Chapter 5, Section 5*. Report AC 43.13-1B. Federal Aviation Administration, U.S. Department of Transportation, Washington, DC, September 1998. http://av-info.faa.gov/dst/43-13/. Accessed August 25, 2003.

24. Stratfull, R. F., W. J. Jurkovich, and D. L. Spellman. Corrosion Testing of Bridge Decks. In *Transportation Research Record 539*, TRB, National Research Council, Washington, DC, 1975, pp. 50-59.

25. Standard Test Method for Half-Cell Potentials of Uncoated Reinforcing Steel in Concrete. ASTM C 876-99. American Society for Testing and Materials, West Conshohocken, PA, 1999, pp. 9-14.

26. Elsener, B. Half-Cell Potential Mapping to Assess Repair Work on RC Structures. In *Construction and Building Materials*, Vol. 15, No. 3, March 2001, pp. 133-139.

27. Standard Test Method for Water Soluble Chloride in Mortar and Concrete. ASTM C 1218-99. American Society for Testing and Materials, West Conshohocken, PA, 1999, pp. 265-66.